By contrast, Tie2 function in BECs has been intensively analyzed at both developmental and adult stages. In vivo and in vitro experiments show that Tie2 signaling potently induces sprouting, chemotaxis, and network formation.[22,23] Furthermore, the Tie2 ligand Ang1 is a potent survival factor for BECs under serum deprivation.[24] A role for Tie2 signaling in blood vessel endothelial survival in vivo has also been illustrated using conditional rescue of $Tie2^{-/-}$ embryos,[25] further supporting a role of this signaling system in endothelial cell survival.

Recently it has been demonstrated in mice that Tie2 is expressed and functions in lymphatic vessels embryonically[26] and in adults.[27] Tie2-deficient mice exhibit severe defects in vascular and heart development and die by E9.5,[28,29] making analysis of the lymphatic system difficult. Therefore, here we analyzed the function of Tie2 in lymphatic endothelial cells (LECs) and hematopoietic cells as well as in developing BECs using differentiation of cultured ES cells. We identify ES cell–derived LECs as well as BECs and hematopoietic cells, and demonstrate that Tie2 signaling is essential for development of BECs and LECs, but not for hematopoietic cells.

Materials and methods

Cell preparation and culture conditions

TT2,[30] E14,[31] and R1[32] ES cells were maintained on mouse embryonic fibroblast (MEF) feeder cell layers in knockout Dulbecco-modified Eagle medium (Gibco BRL, Carlsbad, CA) containing 15% fetal bovine serum (Intergen, Purchase, NY), 100 U/mL leukemia inhibitory factor (LIF; Chemicon International, Temecula, CA), 0.1 mM nonessential amino acids (Gibco BRL), 1 mM sodium pyruvate (Gibco BRL), 2 mM L-glutamine (Gibco BRL), and 100 μM 2-mercaptoethanol (Sigma-Aldrich, St Louis, MO). After removal of LIF, ES cells were cultured on collagen type IV plates (Becton Dickinson, San Jose, CA) at 1×10^4 cells/mL for 2 days. Cells were then disaggregated by trypsin and seeded on OP9 cells at 1×10^5 cells/mL. After 5 days of culture, OP9 cells were removed from ES cells through a Sephadex G10 column (Amersham Bioscience, Uppsala, Sweden), and the ES cells were fractionated by Flk1 and Tie2 expression using FACSvantage (Becton Dickinson). Sorted cells were seeded on OP9 cells at 1000 to 15 000 cells/mL and cultured in the presence of VEGF-C (100 ng/mL; R&D Systems, Minneapolis, MN), VEGF-D (100 ng/mL; R&D Systems), or the caspase inhibitor Z-VAD-fmk (10-100 nM; Calbiochem, La Jolla, CA). When indicated, sorted cells were cultured with recombinant soluble Tie2-Fc fusion protein (30 μg/mL)[19] or recombinant soluble CD4-Fc fusion protein (30 μg/mL).[19]

Immunocytochemistry

Immunocytochemistry was performed essentially as described.[33] Differentiated ES cells cultured on OP9 cells were fixed with 4% paraformaldehyde at 4°C and stained with a rat monoclonal anti-mouse platelet–endothelial cell adhesion molecule 1 (PECAM-1) monoclona antibody (mAb) (MEC13.3; Becton Dickinson) or a rat monoclonal anti-mouse LYVE-1 antibody (ALY7[26]) by the indirect immunoperoxidase method using horseradish peroxidase–conjugated anti-rat IgG. Peroxidase activity was visualized using 3,3'-diaminobenzidine (Dojindo, Kumamoto, Japan). To determine whether Prox-1 was expressed in LYVE-1+ cells, we stained cells with biotinylated ALY7 and anti–Prox-1 antibody (Covance, Berkeley, CA). LYVE-1 and Prox-1 expression was detected by reacting with Alexa 488–conjugated Streptavidin (Molecular Probes, Eugene, OR) and Alexa 546–conjugated goat anti-rabbit antibody (Molecular Probes), respectively. For nuclear staining, cells were treated with TOTO3 (Molecular Probes). Stained cells were visualized by fluorescence microscopy. Stained and unstained cells were visualized by fluorescent microscopy (IX71) with either UplanApo 4×/0.13 NA, 10×/0.40 NA, or 20×/0.70 NA objectives (Olympus, Tokyo, Japan). Images were further processed with Adobe

Photoshop (Adobe Systems, San Jose, CA). For DiI labeling, 10 μg/mL DiI-Ac-LDL (Molecular Probes) was added to differentiated ES cells on OP9 cells and adherent cells were incubated for 4 hours at 37°C. After removing the media containing DiI-Ac-LDL, cells were washed and stained with anti–PECAM-1 (FITC-conjugated; Becton Dickinson) or anti–LYVE-1 (biotin-conjugated) plus FITC-conjugated Streptavidin (Becton Dickinson). Uptake of DiI-Ac-LDL by blood vessel endothelial cells (PECAM-1+ cells) and lymphatic endothelial cells (LYVE-1+ cells) was visualized using a standard rhodamine excitation emission filter (Olympus, Tokyo, Japan).

RT-PCR analysis

Total RNA was extracted from cells using RNeasy Kit (Qiagen, Hilder, Germany). Isolated RNA was reverse-transcribed using an reverse transcriptase (RT) for polymerase chain reaction (PCR) Kit (Clontech, Palo Alto, CA). cDNAs were amplified using Taq polymerase (TaKaRa, Kyoto, Japan). Sequences of gene-specific primers for RT-PCR were as follows: *GATA2*, 5'-(acacaccacccgatacccacctat), 3'-(cctacgccatggcagtcaccatgct); *SCL*, 5'-(cgcggatccacggagcggccgccgagcgcg), 3'-(cggaattccgcgccgcactactt-tggtgtg); c-myb, 5'-(gacagaagaggaggacagaatca), 3'-(tctcagggtcttcgtcgt-tatag); *AML1*, 5'-(ccagcaagctgaggagcggcg), 3'-(cggatttgtaaagacggtga); *Tie2*, 5'-(ttagttctctgtggagtcag), 3'-(aggccctgagttcttcactc); *Flk1*, 5'-(agaacac-caaaagagaggaacg), 3'-(gcacacaggcagaaaccagtag); *VEGFR3*, 5'-(gctaccact-gctactacaag), 3'-(gataatcccagtcgaaggtg); *Prox1*, 5'-(aagtggttcagcaatttccg), 3'-(tgaccttgtaaatggccttc); *LYVE1*, 5'-(ttcctcgcctctatttggac), 3'-(tctgttgtct-gcgtttcatcc); *Pdpn*, 5'-(gtgccagtgttgttctgggt), 3'-(tctgttgtctgcgtttcatcc); *Evi1*, 5'-(aatatgagtcatgccaaccc), 3'-(cttggtgtactgacatcatc); and *GAPDH*, 5'-(aatcccatcaccatcttcca), 3'-(ccaggggtcttactccttg).

PCR products were separated on a 1.2% agarose gel and gels were stained with ethidium bromide.

Quantitative RT-PCR analysis

Total RNA was isolated from 10^4 cells and cDNA was reverse-transcribed using Superscript III (Invitrogen, Carlsbad, CA) according to the manufacturer's instructions. The expression levels of Ang1, Ang2, and Ang3 were analyzed by quantitative (Q) RT-PCR using a LightCycler instrument (Roche Diagnostics, Mannheim, Germany) with LightCycler software version 3.5. cDNA was amplified for Q-PCR using SYBR Green I (Sigma-Aldrich) to detect PCR product. cDNA (2 μL) was used in a 20-μL final volume reaction containing 10 μL SYBR Premix Ex Taq (TaKaRa), 0.4 μM *Ang1* forward (5'-GCCTTTGCACTAAAGAAGGTGTTTT-3'), and 0.4 μM *Ang1* reverse (5'-ATACATCCGCACAGTCTCGAAATG-3'). The LightCycler was programmed to run an initial denaturation step at 95°C for 10 seconds followed by 45 cycles of denaturation (95°C for 5 seconds) and extension (60°C for 20 seconds), monitoring the synthesis of product at the end of the extension step of each cycle. The same conditions were used with primers *Ang2* forward (5'-AGGAGATCAAGGCCTACTGT-GACA-3') and *Ang2* reverse (5'-GCTCCCGAA GCCCTCTTTG-3'), and *Ang3* forward (5'-GTTCCAGGACTGTGCAGAGATCA-3') and *Ang3* reverse (5'-TCTCCATGTCACAGAACACCTTGAG-3'). The Ang1, Ang2, and Ang3 values were normalized against mouse β-actin (forward 5'-CAGCCTTCCTTCT-TGGGTATGG-3'; reverse 5'-CTGTGTTGGCATAGAGGTC TTTACG-3').

Flow cytometric analysis and cell sorting

The following mAbs used for flow cytometry were purchased from Becton Dickinson: anti-CD34 (RAM34), anti–c-Kit (ACK45), anti–Sca-1 (E13-161.7), anti–CD45 (30-F11), anti–Flk1 (Avas12α1), anti–PECAM-1 (MEC13.3), anti–Mac-1 (M1/70), anti–Gr-1 (RB6-8C5), and anti–TER-119. Also used were anti-Tie2 mAb (TEK4)[34] and anti–LYVE-1 mAb (ALY7).[26] Fluorescence-activated cell sorting (FACS) analysis was performed on a FACSvantage (Becton Dickinson).

Progenitor assay by methylcellulose culture

Tie2+Flk1+ or Flk1+ cells derived from ES cells were embedded in 1 mL alpha medium containing 1.3% methylcellulose (1500 cp; Sigma-Aldrich), 30% fetal calf serum (FCS), 1% deionized bovine serum albumin (BSA;

Sigma-Aldrich), 0.1 mM 2-mercapto-ethanol (Sigma-Aldrich), 10 ng/mL stem cell factor (SCF; PeproTech EC, London, United Kingdom), 10 ng/mL recombinant mouse interleukin-3 (IL-3; PeproTech EC), 10 ng/mL recombinant human IL-6 (PeproTech EC), and 2 U/mL recombinant human erythropoietin (Epo; Chugai Pharmaceutical, Tokyo, Japan). Cells were cultured in a 35-mm culture dish and incubated at 37°C in a humidified atmosphere with 5% CO_2.

Statistics

Data are expressed as means plus or minus standard deviation (SD). Statistical analysis was conducted using the Student t test. Statistical significance was defined as a P value less than .05.

Results

In vitro differentiation of ES cells

In order to analyze the function of Tie2 in the development of LECs as well as BECs and hematopoietic cells, we developed a cell culture system for ES cell differentiation. After removal of LIF, E14 ES cells were cultured on collagen type IV plates for 2 days to initiate differentiation to a mesoderm lineage; subsequently, cells were transferred to OP9 stromal cells. Markers of both endothelial and hematopoietic cells, Sca-1, c-kit, and CD34, were expressed in undifferentiated ES cells (Figure 1A). Although 1% of ES cells expressed Flk1 on collagen plates, Tie2 was not expressed in Flk1^{+}
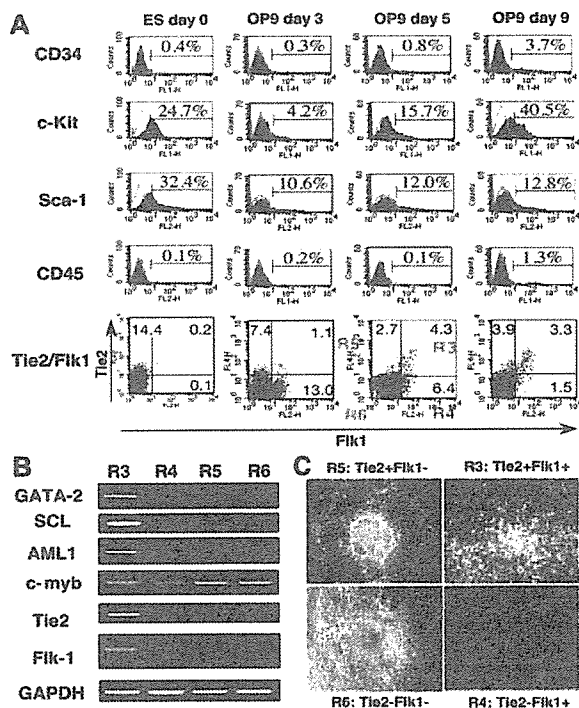

Figure 1. Mesodermal differentiation of ES cells on OP9 stromal cells. (A) E14 ES cells were cultured on collagen type IV plates for 2 days, and then all cells were cultured on OP9 cells for 9 days. The expression of CD34, c-Kit, Sca-1, CD45, Flk1, and Tie2 in ES cell–derived cells was analyzed at the indicated time points by flow cytometry. Stained Tie^{−/−} cells are represented by purple shaded histograms. Unstained controls are represented by green lines. The percentages of cells in each quadrant are indicated. (B) Gene expression of fractionated cells shown in A (R3-R6) was analyzed by RT-PCR. (C) Fractionated cells (20 000; R3-R6) were cultured on OP9 cells. On day 7 of culture, hematopoietic clusters (red arrowheads) were developed only from the R3 fraction. In other fractions (R4-R6) hematopoietic clusters were not developed, but embryoid body–like colonies (blue arrowheads) developed from R5 and R6 fractions. Cells were analyzed at low (×40) magnification.
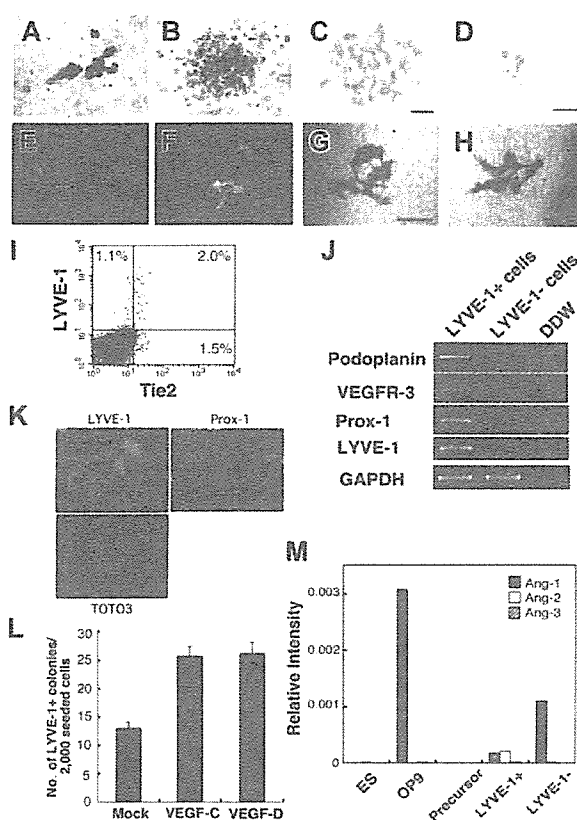
cells (data not shown). Following transfer of cells on collagen plates to OP9 cells, 8% of Flk1^{+} cells expressed Tie2 on day 3 of culture. Numbers of Tie2^{+} cells increased until day 5 of culture, when Tie2 expression was maximal; thereafter, both expression levels and numbers of Tie2^{+} cells gradually decreased. At day 9 of culture, cells cocultured with OP9 cells began expressing CD45, a marker of all hematopoietic cells except mature erythrocytes. Since Tie2^{+} cells appeared just before CD45^{+} hematopoietic cells, Tie2^{+} cells in the Flk1^{+} cell fraction may represent hematopoietic progenitor cells. We examined other ES strains, such as TT2 and R1 cells, using the same culture conditions, and confirmed that these strains showed a similar mesodermal phenotypes as E14 cells (data not shown).

Development of hematopoietic, lymphatic endothelial, and blood vessel endothelial cells from Flk1^{+}Tie2^{+} cells

To analyze the differentiating potential of ES-derived cells, we fractionated cells on day 5 of culture using Tie2 and Flk1 mAb as shown in Figure 1A (bottom panel, R1-R4). Expression profiling of transcription factors specific for hematopoietic or endothelial cells was undertaken by RT-PCR (Figure 1B). Expression levels of GATA-2, SCL, and AML-1 in the Tie2^{+}Flk1^{+} fraction (R3) were 1.7-, 2.5-, and 1.7-fold higher than those in the Tie2^{−}Flk1^{+} fraction (R4), respectively. In the Flk1^{−} fraction (R5 and R6), expression levels of these genes were much lower compared with the Tie2^{−}Flk1^{+} fraction (R4), suggesting that the Tie2^{+}Flk1^{+} fraction may contain committed progenitors of hematopoietic and endothelial lineages. Cells (20 000) fractionated by Flk1 and Tie2 expression were cultured on OP9 cells (Figure 1C), and hematopoietic clusters formed only from the Tie2^{+}Flk1^{+} fraction (R3) (Figure 1C, red arrowheads). Hematopoietic clusters were not detected in Flk1^{+}Tie2^{−} (R4), Flk1^{−}Tie2^{+} (R5), or Flk1^{−}Tie2^{−} fractions (R6). The number of hematopoietic progenitors in each fraction was estimated by colony-forming assays in methylcellulose culture (Figure 2A-B). BECs were detected by staining with PECAM-1 mAb (Figure 2C). PECAM-1^{+} endothelial cells were spindle shaped and took up an acetyl-LDL (Figure 2D). To detect LECs, we generated a mAb against LYVE-1 (ALY7), a receptor for extracellular matrix glycosaminoglycan. Using this mAb, we detected LYVE-1^{+} cells on OP9 cells (Figure 2E). These cells also took up acetyl-LDL (Figure 2F), and 65% of them expressed Tie2 (Figure 2I). The lymphatic identity of these cells was further demonstrated by RT-PCR, using primers specific for LEC-enriched genes, namely, Pdpn, VEGFR3, and Prox1 (Figure 2J). Furthermore, LYVE-1^{+} cells coexpressed Prox-1 (Figure 2K). The presence of VEGFR-3 transcripts in these cultures provided the impetus for us to add the lymphatic growth factors, VEGF-C and VEGF-D. The addition of these factors resulted in a marked increase in the number of LYVE-1^{+} cells (Figure 2L) and an increase in the size of monolayers (VEGF-C, Figure 2G; VEGF-D, Figure 2H). These findings suggest that LYVE-1^{+} cells derived from ES cell differentiation cultures express many genes that are restricted to or enriched in LECs.

That Tie2 is required for these cell types is supported by the more than 10-fold increase in hematopoietic, blood vessel endothelial, and lymphatic endothelial colonies from Tie2^{+}Flk1^{+} cells compared with Tie2^{−}Flk1^{+} or Tie2^{−}Flk1^{−} cell fractions (Table 1). To determine which cells produce the Tie2 ligands Ang1, Ang2, and Ang3 in order to support Tie2^{+} cells, we performed quantitative expression analysis for Ang1, Ang2, and Ang3. As shown in Figure 2M, OP9 cells and LYVE-1^{−} ES-derived cells expressed Ang1 but not Ang2 or Ang3. Although low expression levels of

Figure 2. Development of lymphatic endothelial cells from ES cells. The Tie2⁺Flk1⁺ fraction of ES cell–derived cells formed erythroid colonies (A) and granulocyte-macrophage colonies (B) in methylcellulose. Vascular and lymphatic endothelial cells were stained with PECAM-1 mAb (C) and LYVE-1 mAb (D), respectively. PECAM-1⁺ cells (green, panel E) and LYVE-1⁺ cells (green, panel F) took up acetyl-LDL (red, panels E and F). Scale bars, 10 μm. (I) Expression of LYVE-1 and Tie2 in differentiated cells derived from ES cells on OP9 cells on day 6 of culture was analyzed by flow cytometry. The percentages of cells in each quadrant are indicated. (J) Lymphatic-specific genes, Pdpn, VEGFR-3, and Prox-1 in LYVE-1⁺ and LYVE-1⁻ cells were analyzed by RT-PCR. (K) Immunostaining at high magnification (× 200) showed that LYVE-1⁺ cells (green) coexpressed Prox-1 (red). TOTO3 (blue) was used to stain nuclei. (L) In the presence of VEGF-C and VEGF-D (100 ng/mL each), the number of LYVE-1⁺ colonies increased to 2 times that of mock-treated cells. Colonies were also larger in the presence of VEGF-C and VEGF-D (panels G and H, respectively). Results are expressed as the mean ± SD. (M) OP9 and ES cell–derived LYVE-1⁻ cells expressed Ang1. LYVE-1⁺ cells expressed low levels of Ang1 and Ang2. Ang1, Ang2, and Ang3 were not detectable in ES cells and lymphatic precursors (Flk1⁺ cells derived from ES cells).

Ang1 and Ang2 were detected in LYVE-1⁺ cells, ES cells and lymphatic precursor cells (ES cell–derived Flk1⁺ cells) did not express Ang's. These results suggest that Ang1 derived from OP9 cells might affect the growth or survival of Tie2⁺ cells.

Table 1. Frequency of hematopoietic and endothelial progenitors of differentiated ES cells

	Erythroid colonies from 30 000 cells	GM colonies from 30 000 cells	Vascular endothelial colonies from 1500 cells	Lymphatic endothelial colonies from 2000 cells
Tie2⁺Flk1⁺	11.3 ± 6.4	11.7 ± 2.1	47.5 ± 5.3	24.3 ± 2.5
Tie2⁻Flk1⁺	0	0	5.2 ± 1.8	0
Tie2⁺Flk1⁻	0	0	0	0
Tie2⁻Flk1⁻	0	0	0	0
Bulk	0	0	2.7 ± 1.5	1.3 ± 0.6

Development of hematopoietic and endothelial cells from Tie2-deficient ES cells

To clarify the function of Tie2 during hematopoietic and endothelial differentiation from ES cells, the differentiation capacity of $Tie2^{-/-}$ ES cells was examined using our culture system. $Tie2^{-/-}$ ES cells grew normally on MEF feeder layer cells (data not shown), and differentiated cells grown on OP9 cells were analyzed by flow cytometry. The frequency of cells expressing Flk1 in the $Tie2^{-/-}$ ES cells was similar to that seen in $Tie2^{+/-}$ cells (Figure 3A). RT-PCR of RNA from this fraction for expression of the genes involved in development of hematopoietic and endothelial cells revealed no remarkable differences between $Tie2^{+/-}$ and $Tie2^{-/-}$ cells (Figure 3B). To analyze hematopoietic development of $Tie2^{-/-}$ ES cells, we calculated the number of hematopoietic clusters formed on OP9 cells at day 7 of culture. The number and size of hematopoietic clusters of $Tie2^{-/-}$ ES cells were the same as those of $Tie2^{+/-}$ cells (Figure 3C, and data not shown). When the $Tie2^{-/-}$ hematopoietic clusters were transferred to fresh OP9 cells for an additional week, normal proliferating hematopoietic cells were detected by flow cytometry. Mature Mac-1–, Gr-1–, and Ter119–positive hematopoietic cells were differentiated from $Tie2^{-/-}$ ES cells (Figure 3D), and the frequency of mature hematopoietic cells was similar to that seen in $Tie2^{+/-}$ cells (data not shown), suggesting that Tie2 is not essential for development of hematopoietic cells. By contrast, $Tie2^{-/-}$ ES cells were severely defective in forming blood vessel and lymphatic endothelial colonies on OP9 cells at day 6 of culture. The number of such blood vessel and lymphatic endothelial colonies was approximately one
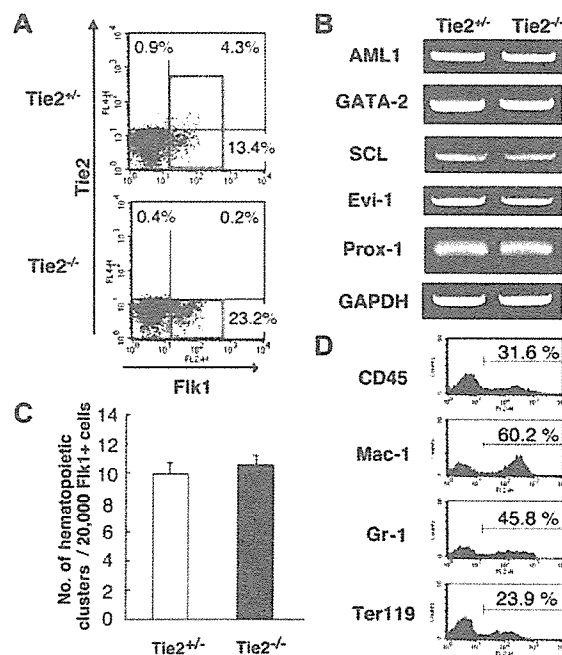

Figure 3. Normal development of hematopoietic cells from $Tie2^{-/-}$ ES cells. (A) FACS analysis of the expression of Flk1 and Tie2 in $Tie2^{-/-}$ and $Tie2^{+/-}$ ES cell-differentiated cells. Red squares show the Flk1⁺ fraction. The percentages of cells in each quadrant are indicated. (B) Expression of genes associated with mesoderm in Flk1⁺ cells shown in panel A (red squares) was analyzed by RT-PCR. (C) Flk1⁺ cells (20 000) were cultured on OP9 cells. The number of hematopoietic clusters from $Tie2^{+/-}$ and $Tie2^{-/-}$ cells at day 7 of culture was calculated. Results are expressed as the mean ± SD. (D) $Tie2^{-/-}$ hematopoietic clusters were cultured for an additional 7 days on fresh OP9 cells. The expression of CD45, Mac-1, Gr-1, and Ter119 was analyzed by flow cytometry. ES cell–derived hematopoietic cells are represented by purple shaded histograms; unstained controls, by green lines.
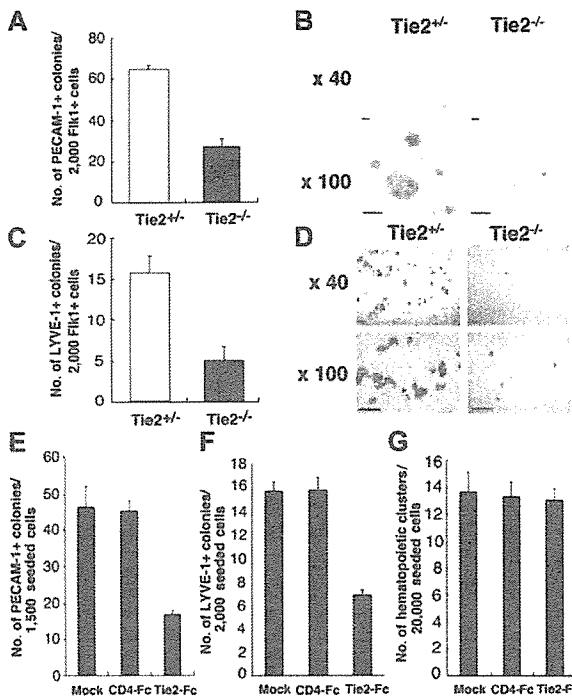
Figure 4. Lymphatic and blood vessel endothelial cell development from Tie2$^{-/-}$ ES cells. (A) Flk1$^+$ cells (2000) were cultured on OP9 cells. At day 7 of culture, the number of vascular endothelial colonies developed from Tie2$^{+/-}$ (□) and Tie2$^{-/-}$ (■) ES cells was calculated. (B) Vascular endothelial colonies were stained with PECAM-1 mAb and analyzed at low (× 40) and high (× 100) magnification. (C) The number of lymphatic endothelial colonies developed from Tie2$^{+/-}$ (□) and Tie2$^{-/-}$ (■) ES cells was calculated. (D) Lymphatic endothelial colonies were stained with LYVE-1 mAb and analyzed at low (× 40) and high (× 100) magnification. Scale bars in panels B and D, 20 μm. In the presence of Tie2-Fc (30 μg/mL), the number of vascular and lymphatic endothelial colonies was decreased (panels E and F, respectively). (G) Hematopoietic cluster formation was not affected by exogenous soluble Tie2-Fc (30 μg/mL). Exogenous soluble CD4-Fc (30 μg/mL) served as the control. Results in panels A, C, and E-G are expressed as the mean ± SD.

third that observed from Tie2$^{+/-}$ cells (Figure 4A-B), and colony size was smaller than that seen from Tie2$^{+/-}$ cells (Figure 4C-D). These results suggest that Tie2 function is required for development of BECs and LECs, but not of hematopoietic cells. To confirm these findings, we added soluble Tie2-Fc fusion protein to the culture media of wild-type ES cells to block Tie2 signaling. As shown in Figure 4E-G, the number of vascular and lymphatic endothelial cell colonies derived from wild-type ES cells in the presence of soluble Tie2-Fc fusion protein decreased to one half to one third of the mock-treated cells, while the number of hematopoietic clusters was not affected by soluble Tie2-Fc fusion protein. We did not detect such inhibition in the presence of soluble CD4-Fc fusion protein (Figure 4 E-F).

Tie2 signaling is crucial for antiapoptotic signaling in the development of lymphatic and blood vessel endothelial cells

To further analyze the mechanisms underlying defective proliferation of BECs and LECs from Tie2$^{-/-}$ ES cells, we analyzed expression of blood vessel- and lymphatic-specific markers PECAM-1 and LYVE-1, respectively, by flow cytometry at days 2, 4, and 6 of culture (Figure 5A). Cells expressing PECAM-1 and LYVE-1 in Tie2$^{-/-}$ ES cells decreased over 6 days. PECAM-1$^+$ cells in Tie2$^{-/-}$ cells were approximately one third the number of those in Tie2$^{+/-}$ cells at day 6 of culture, as was the case with LYVE-1$^+$ cells (Figure 5B-C). This finding suggested that Tie2$^{-/-}$-mediated signaling

protects endothelial cells from cell death. To test this possibility, we treated Tie2$^{-/-}$ cells with the caspase inhibitor Z-VAD-fmk. As shown in Figure 5B and C, lymphatic and blood vessel endothelial colony formation was rescued in the presence of Z-VAD-fmk in a dose-dependent fashion. In the presence of 50 nM of Z-VAD-fmk, the number of lymphatic endothelial colonies from Tie2$^{-/-}$ cells was rescued to 60% of that from Tie2$^{+/-}$ cells (Figure 5C), although the size of Tie2$^{-/-}$ lymphatic endothelial colonies remained small (Figure 5D). The formation of blood vessel endothelial colonies was similar in the presence of Z-VAD-fmk (50 nM; Figure 5C). These findings suggest that Tie2 signaling is crucial for LEC and BEC development and mediates antiapoptotic signaling during ES cell differentiation.

Discussion

Although we have demonstrated that Tie2 is expressed in the vitelline artery,[19] the AGM region,[4] and fetal liver,[20] the function of Tie2 in development has not been elucidated. The early death of Tie2$^{-/-}$ embryos precludes detailed analysis of the role of Tie2 in
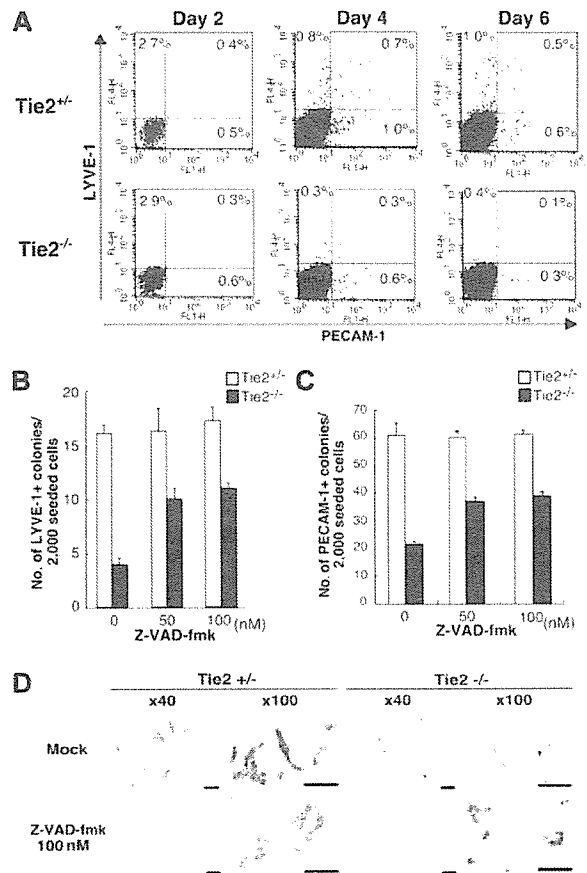

Figure 5. Tie2 signaling in blood vessels and lymphatic endothelial cells protected from apoptosis. (A) Expression of PECAM-1 and LYVE-1 in ES cell–derived cells was analyzed by flow cytometry at days 2, 4, and 6 of culture. The percentages of cells in each quadrant are indicated. (B) Addition of the caspase inhibitor Z-VAD-fmk (50 nM) to the culture media rescued the number of LYVE-1$^+$ colonies from Tie2$^{-/-}$ ES cells (■). (C) The number of PECAM-1$^+$ colonies from Tie2$^{-/-}$ ES cells (■) was also rescued in the presence of Z-VAD-fmk (50 nM). Results are expressed as mean ± SD. (D) In the presence of Z-VAD-fmk, the size of Tie2$^{-/-}$ lymphatic endothelial cells was unchanged, although the number of lymphatic colonies was partially rescued. Scale bars, 20 μm.

development of hematopoietic and endothelial lineages. Using an ES cell differentiation system, we have analyzed the development of hematopoietic cells as well as BECs and LECs from $Tie2^{-/-}$ ES cells. At day 8 of culture on OP9 cells, the normal formation of hematopoietic clusters from $Tie2^{-/-}$ cells suggests that Tie2 signaling does not contribute to development of hematopoietic cells from precursors. Furthermore, differentiation of myeloid cells from $Tie2^{-/-}$ hematopoietic clusters was normal. These results indicate that Tie2 is not essential for development of hematopoietic cells from ES cells. Recently, Puri and Bernstein[21] used combined mosaic analysis to demonstrate that Tie receptors are not required for differentiation and proliferation of definitive hematopoietic lineages in the embryo and fetus. Their findings are consistent with what we show in this study. Although our in vitro differentiation experiments suggest that Tie2 is not essential for hematopoiesis during development, Ang1/Tie2 signaling in hematopoietic cells has been reported to function to maintain hematopoietic stem cells in the bone marrow niche where Ang1 is expressed by osteoblasts.[18] Thus Tie2 function in hematopoiesis would seem to be specific for adult bone marrow.

Although much is known about normal and pathologic development of the vascular system,[35] the lack of specific markers has made it difficult to follow the development of the lymphatic system. In order to identify LECs, we recently generated a LEC-specific mAb against LYVE-1.[26] This mAb allowed us to detect LECs in mouse embryos at midgestation and purify these cells. ES cell–derived LYVE-1^{+} cells express LEC-specific genes, such as *Prox1*, *Pdpn*, and *VEGFR3*, and exhibit DiI-Ac-LDL uptake. Furthermore, VEGF-C and VEGF-D, lymphatic growth factors, increased the number of LYVE-1–positive endothelial colonies from ES cells. These findings indicate that LYVE-1^{+} cells isolated from these cultures have many characteristics of LECs. Lymphatic vasculature of the thoracic and abdominal viscera have been proposed to arise by endothelial spreading from lymph sacs.[6,36] This proposal is supported by the finding that budding of endothelial cells from the veins of Prox-1 mutant embryos is arrested.[9,10] To clarify the mechanisms of lymphangiogenesis in vitro, we analyzed the function of Tie2. In this study LECs were differentiated from ES cell–derived Tie2^{+}Flk1^{+} cells, and approximately 1% of Tie2^{+}Flk1^{+} cells formed lymphatic endothelial colonies on OP9 cells. Our in vitro differentiation assay allows us to clarify the mechanisms of LEC development from its precursor.

Thus far, Tie2 signaling has been reported to be required for proper development and function of the vascular system. Mice lacking Ang2 exhibit lymphatic vessel defects, strongly suggesting a role of Tie2 signaling in lymphangiogenesis.[37] In this study we have shown that LECs and BECs can be differentiated from Tie2^{+}Flk1^{+} cells, and that 65% of LYVE-1^{+} LECs express Tie2. To analyze the function of Tie2 in the development of lymphatic

endothelial cells, we performed FACS analysis and immunocytochemistry during differentiation of $Tie2^{-/-}$ ES cells. FACS analysis revealed that $Tie2^{-/-}$ cells expressing LYVE-1 decreased over time as did PECAM-1^{+} BECs. Treatment with a caspase inhibitor, which specifically inhibits apoptosis, partially rescued defective formation of lymphatic and blood vessel endothelial colonies from $Tie2^{-/-}$ cells, suggesting that both endothelial cells undergo apoptosis in the absence of Tie2 signaling. Although Tie2 signaling contributed to the survival of both LECs and BECs on OP9 cells, treatment with the caspase inhibitor did not affect the size of $Tie2^{-/-}$ colonies. Based on these findings, we propose that Tie2 cooperates with other signaling pathways involved in growth. Although we do not identify these pathways, OP9 cells are known to secrete several growth factors, including VEGF-C and VEGF-D.[38] FACS analysis also revealed that at day 2 of culture, the frequency of LYVE-1^{+} and PECAM-1^{+} cells derived from $Tie2^{-/-}$ cells was comparable with frequencies seen in $Tie2^{+/-}$ cells, suggesting that lymphatic and blood vessel endothelial precursors develop normally from $Tie2^{-/-}$ cells. A gene expression study clearly showed that expression levels of Prox-1 in lymphatic precursors (the Flk1^{+} cell fraction) of $Tie2^{-/-}$ cells were comparable with those seen in $Tie2^{+/-}$ cells, suggesting that Tie2 deficiency does not affect Prox-1 expression. These findings suggest that Tie2 is not essential for development of lymphatic and blood vessel endothelial precursors, although both types of endothelial cells from $Tie2^{-/-}$ cells undergo apoptosis due to lack of Tie2 signaling.

Regarding vascular endothelial cells, in vivo study has shown that mice lacking Ang1 and Tie2 develop a fairly normal primary vasculature, but that this vasculature fails to undergo further normal remodeling.[28,39,40] We have demonstrated that lymphatic endothelial cells express Tie2 in both embryonic and adult settings, and that the activation of Tie2 signaling by Ang1 stimulates both in vivo lymphatic angiogenesis in mouse cornea and in vitro colony formation of lymphatic endothelial cells.[26] Data from both in vitro ES cell differentiation and in vivo embryonic development suggest that Ang/Tie2 signaling may contribute to regulation of lymphatic vessel formation in the development of lymphatic vessels.

In summary, our results derived from induction studies of ES cells have revealed that Tie2 is expressed in the precursors of mesodermal lineages, hematopoietic cells, and endothelial cells. We have also shown that Tie2 is not essential for development of hematopoietic cells, but that it plays an important role in antiapoptotic signaling in lymphatic and blood vessel development.

Acknowledgment

References

1. Sabin F. Studies on the origin of blood vessels and red corpuscles as seen in the living blastoderm of the chick during the second day of incubation. Contribut Embryol. 1920;9:213-262.

2. Kubo H, Alitalo K. The bloody fate of endothelial stem cells. Genes Dev. 2003;17:322-329.

3. Haar JL, Ackerman GA. A phase and electron microscopic study of vasculogenesis and erythropoiesis in the yolk sac of the mouse. Anat Rec. 1971;170:199-223.

4. Hamaguchi I, Huang XL, Takakura N, et al In vitro hematopoietic and endothelial cell development from cells expressing TEK receptor in murine

aorta-gonad-mesonephros region. Blood. 1999; 93:1549-1556.

5. Choi K, Kennedy M, Kazarov A, Papadimitriou JC, Keller G. A common precursor for hematopoietic and endothelial cells. Development. 1998; 125:725-732.

6. Sabin FR. On the origin of the lymphatic system from the veins, and the development of the lymph hearts and thoracic duct in the pig. Am J Anat. 1902;1:367-389.

7. Oliver G, Detmar M. The rediscovery of the lymphatic system: old and new insights into the development and biological function of the lymphatic vasculature. Genes Dev. 2002;16:773-783.

8. Jeltsch M, Kaipainen A, Joukov V, et al. Hyperplasia of lymphatic vessels in VEGF-C transgenic mice. Science. 1997;276:1423-1425.

9. Wigle JT, Oliver G. Prox1 function is required for the development of the murine lymphatic system. Cell. 1999;98:769-778.

10. Wigle JT, Harvey N, Detmar M, et al. An essential role for Prox1 in the induction of the lymphatic endothelial cell phenotype. EMBO J. 2002;21: 1505-1513.

11. Shalaby F, Rossant J, Yamaguchi TP, et al. Failure of blood-island formation and vasculogenesis in Flk-1-deficient mice. Nature. 1995;376:62-66.

12. Shalaby F, Ho J, Stanford WL, et al. A require-
ment for Flk1 in primitive and definitive hemato-
poiesis and vasculogenesis. Cell. 1997;89:981-
990.

13. Millauer B, Wizigmann-Voos S, Schnurch H, et al.
High affinity VEGF binding and developmental
expression suggest Flk-1 as a major regulator of
vasculogenesis and angiogenesis. Cell. 1993;72:
835-846.

14. Dumont DJ, Fong GH, Puri MC, Gradwohl G, Ali-
talo K, Breitman ML. Vascularization of the
mouse embryo: a study of flk-1, tek, tie, and vas-
cular endothelial growth factor expression during
development. Dev Dyn. 1995;203:80-92.

15. de Vries C, Escobedo JA, Ueno H, Houck K, Fer-
rara N, Williams LT. The fms-like tyrosine kinase,
a receptor for vascular endothelial growth factor.
Science. 1992;255:989-991.

16. Dumont DJ, Gradwohl GJ, Fong GH, Auerbach
R, Breitman ML. The endothelial-specific receptor
tyrosine kinase, tek, is a member of a new sub-
family of receptors. Oncogene. 1993;8:1293-
1301.

17. Iwama A, Hamaguchi I, Hashiyama M, Murayama
Y, Yasunaga K, Suda T. Molecular cloning and
characterization of mouse TIE and TEK receptor
tyrosine kinase genes and their expression in he-
matopoietic stem cells. Biochem Biophys Res
Commun. 1993;195:301-309.

18. Arai F, Hirao A, Ohmura M, et al. Tie2/angiopoi-
etin-1 signaling regulates hematopoietic stem cell
quiescence in the bone marrow niche. Cell. 2004;
118:149-161.

19. Takakura N, Huang XL, Naruse T, et al. Critical
role of the TIE2 endothelial cell receptor in the
development of definitive hematopoiesis. Immu-
nity. 1998;9:677-686.

20. Hsu HC, Ema H, Osawa M, Nakamura Y, Suda T,
Nakauchi H. Hematopoietic stem cells express
Tie-2 receptor in the murine fetal liver. Blood.
2000;96:3757-3762.

21. Puri MC, Bernstein A. Requirement for the TIE

family of receptor tyrosine kinases in adult but not
fetal hematopoiesis. Proc Natl Acad Sci U S A.
2003;100:12753-12758.

22. Koblizek TI, Weiss C, Yancopoulos GD, Deutsch
U, Risau W. Angiopoietin-1 induces sprouting an-
giogenesis in vitro. Curr Biol. 1998;8:529-532.

23. Papapetropoulos A, Garcia-Cardena G, Dengler
TJ, Maisonpierre PC, Yancopoulos GD, Sessa
WC. Direct actions of angiopoietin-1 on human
endothelium: evidence for network stabilization,
cell survival, and interaction with other angiogenic
growth factors. Lab Invest. 1999;79:213-223.

24. Kwak HJ, So JN, Lee SJ, Kim I, Koh GY. Angio-
poietin-1 is an apoptosis survival factor for endo-
thelial cells. FEBS Lett. 1999;448:249-253.

25. Jones N, Voskas D, Master Z, Sarao R, Jones J,
Dumont DJ. Rescue of the early vascular defects
in Tek/Tie2 null mice reveals an essential survival
function. EMBO Rep. 2001;2:438-445.

26. Morisada T, Oike Y, Yamada Y, et al. Angiopoi-
etin-1 promotes LYVE-1-positive lymphatic vessel
formation. Blood. 2005;105:4649-4656.

27. Tammela T, Saaristo A, Lohela M, et al. Angiopoi-
etin-1 promotes lymphatic sprouting and hyper-
plasia. Blood. 2005;105:4624-4648.

28. Dumont DJ, Gradwohl G, Fong GH, et al Domi-
nant-negative and targeted null mutations in the
endothelial receptor tyrosine kinase, tek, reveal a
critical role in vasculogenesis of the embryo.
Genes Dev. 1994;8:1897-1909.

29. Puri MC, Rossant J, Alitalo K, Bernstein A, Par-
tanen J. The receptor tyrosine kinase TIE is re-
quired for integrity and survival of vascular endo-
thelial cells. EMBO J. 1995;14:5884-5891.

30. Yagi T, Tokunaga T, Furuta Y, et al. A novel ES
cell line, TT2, with high germline-differentiating
potency. Anal Biochem. 1993;214:70-76.

31. Hooper M, Hardy K, Handyside A, Hunter S,
Monk M. HPRT-deficient (Lesch-Nyhan) mouse
embryos derived from germline colonization by
cultured cells. Nature. 1987;326:292-295.

32. Nagy A, Rossant J, Nagy R, Abramow-Newerly
W, Roder JC. Derivation of completely cell cul-
ture-derived mice from early-passage embryonic
stem cells. Proc Natl Acad Sci U S A. 1993;90:
8424-8428.

33. Takakura N, Yoshida H, Ogura Y, Kataoka H,
Nishikawa S. PDGFR alpha expression during
mouse embryogenesis: immunolocalization ana-
lyzed by whole-mount immunohistostaining using
the monoclonal anti-mouse PDGFR alpha anti-
body APA5. J Histochem Cytochem. 1997;45:
883-893.

34. Yano M, Iwama A, Nishio H, Suda J, Takada G,
Suda T. Expression and function of murine recep-
tor tyrosine kinases, TIE and TEK, in hematopoi-
etic stem cells. Blood. 1997;89:4317-4326.

35. Gale NW, Yancopoulos GD. Growth factors acting
via endothelial cell-specific receptor tyrosine ki-
nases: VEGFs, angiopoietins, and ephrins in vas-
cular development. Genes Dev. 1999;13:1055-
1066.

36. Gray H. In Anatomy of the human body. In: Clem-
ente CD, ed. The Lymphatic System. Philadel-
phia, PA: Lea and Febiger; 1985:866-932.

37. Gale NW, Thurston G, Hackett SF, et al. Angio-
poietin-2 is required for postnatal angiogenesis
and lymphatic patterning, and only the latter role
is rescued by Angiopoietin-1. Dev Cell. 2002;3:
411-423.

38. Matsumura K, Hirashima M, Ogawa M, et al.
Modulation of VEGFR-2-mediated endothelial-
cell activity by VEGF-C/VEGFR-3. Blood. 2003;
101:1367-1374.

39. Suri C, Jones PF, Patan S, et al. Requisite role of
angiopoietin-1, a ligand for the TIE2 receptor, dur-
ing embryonic angiogenesis. Cell. 1996;87:1171-
1180.

40. Sato TN, Tozawa Y, Deutsch U, et al. Distinct
roles of the receptor tyrosine kinases Tie-1 and
Tie-2 in blood vessel formation. Nature. 1995;
376:70-74.

Loss of Tie2 receptor compromises embryonic stem cell–derived endothelial but not hematopoietic cell survival

Isao Hamaguchi, Tohru Morisada, Masaki Azuma, Kyoko Murakami, Madoka Kuramitsu, Takuo Mizukami, Kazuyuki Ohbo, Kazunari Yamaguchi, Yuichi Oike, Daniel J. Dumont, and Toshio Suda

Tie2 is a receptor-type tyrosine kinase expressed on hematopoietic stem cells and endothelial cells. We used cultured embryonic stem (ES) cells to determine the function of Tie2 during early vascular development and hematopoiesis. Upon differentiation, the ES cell–derived Tie2+Flk1+ fraction was enriched for hematopoietic and endothelial progenitor cells. To investigate lymphatic differentiation, we used a monoclonal antibody against LYVE-1 and found that LYVE-1+ cells derived from Tie2+Flk1+ cells possessed various characteristics of lymphatic endothelial cells. To determine whether Tie2 played a role in this process, we analyzed differentiation of Tie2−/− ES cells. Although the initial numbers of LYVE-1+ and PECAM-1+ cells derived from Tie2−/− cells did not vary significantly, the number of both decreased dramatically upon extended culturing. Such decreases were rescued by treatment with a caspase inhibitor, suggesting that reductions were due to apoptosis as a consequence of a lack of Tie2 signaling. Interestingly, Tie2−/− ES cells did not show measurable defects in development of the hematopoietic system, suggesting that Tie2 is not essential for hematopoietic cell development. (Blood. 2006;107:1207-1213)

© 2006 by The American Society of Hematology

Introduction

A close cell lineage relationship between hematopoietic and endothelial cells has long been recognized.[1,2] During embryogenesis, both cell types emerge in the yolk sac, and primitive erythrocytes differentiate juxtaposed to endothelial precursors by embryonic day 7.5 (E7.5).[3] In the mouse embryo, Tie2+ cells in the aorta-gonad-mesonephros (AGM) region generate both blood and endothelial cells.[4] From studies of embryonic stem (ES) cell differentiation, vascular endothelial growth factor (VEGF)–responsive bipotent precursors of hematopoietic and endothelial cells, known as hemangioblasts, have been identified.[5] Hemangioblast-derived endothelial cells form vascular vessels through vasculogenesis and angiogenesis. Lymphatic development starts when a subset of vascular endothelial cells of the cardinal vein commit to a lymphatic lineage and sprout to form the primary lymph sacs at around E9 or 10.[6,7] Mouse molecular genetic experiments indicate that Prox-1 (a homeobox transcription factor) and the VEGF receptor 3 (VEGFR-3) are crucial for the commitment of endothelial cells to a lymphatic lineage.[8-10] Since lymphatic vessel–specific molecules are being identified, the molecular mechanisms underlying development of lymphatic cells as well as vascular and hematopoietic cells can now be analyzed.

Many studies report that expression of Flk1 is crucial for early establishment of endothelial and hematopoietic lineages and perhaps for their common progenitor.[5,11,12] Flk1 encodes a receptor tyrosine kinase for the vascular endothelial growth factor family of ligands.[13] Single Flk1+ cells from embryoid bodies can give rise to blast colonies (blast lymphocyte colony-forming cells [BL-CFCs]), which produce both hematopoietic and endothelial cells in vitro.[5] Loss of Flk1 in mice results in selective defects in generating both blood and blood-vessel endothelial cells (BECs).[11] In addition to Flk1, Flt1 and Tie2 tyrosine kinases are also expressed in immature hematopoietic cells and BECs.[14-17]

The expression pattern of Tie2 suggests a function in both vascular endothelial and hematopoietic cells. Recently we determined the function of Ang1/Tie2 signaling, which maintains long-term repopulating hematopoietic stem cells in the bone marrow niche, suggesting that Tie2 signaling is crucial for adult bone marrow hematopoiesis.[18] In the mouse vitelline artery at E9.5, Tie2+ hematopoietic cells aggregate and adhere to endothelial cells.[19] In vitro culture of Tie2+ cells isolated from the AGM region generates both blood and endothelial cells.[4] In fetal liver, the Tie2+ fraction contains an enriched fraction of long-term repopulating cells.[20] Based on these findings, Tie2 signaling was thought to regulate embryonic development and differentiation of hematopoietic cells. However, more recently, Puri and Berstein have demonstrated that Tie2 is dispensable for embryonic hematopoiesis using ES cell mouse chimeras.[21] This finding suggests that Tie2 function in developmental hematopoiesis differs from its role in bone marrow hematopoiesis.

Reprints: Isao Hamaguchi, Department of Safety Research on Blood and Biological Products, National Institute of Infectious Diseases, 4-7-1 Gakuen, Musashimurayama, Tokyo 208-0011, Japan; e-mail: 130hama@nih.go.jp; or Toshio Suda, The Sakaguchi Laboratory of Developmental Biology School of Medicine, Keio University, Shinanomachi 35, Shinjuku, Tokyo 160-8582, Japan; e-mail: sudato@sc.itc.keio.ac.jp.

By contrast, Tie2 function in BECs has been intensively analyzed at both developmental and adult stages. In vivo and in vitro experiments show that Tie2 signaling potently induces sprouting, chemotaxis, and network formation.[22,23] Furthermore, the Tie2 ligand Ang1 is a potent survival factor for BECs under serum deprivation.[24] A role for Tie2 signaling in blood vessel endothelial survival in vivo has also been illustrated using conditional rescue of $Tie2^{-/-}$ embryos,[25] further supporting a role of this signaling system in endothelial cell survival.

Recently it has been demonstrated in mice that Tie2 is expressed and functions in lymphatic vessels embryonically[26] and in adults.[27] Tie2-deficient mice exhibit severe defects in vascular and heart development and die by E9.5,[28,29] making analysis of the lymphatic system difficult. Therefore, here we analyzed the function of Tie2 in lymphatic endothelial cells (LECs) and hematopoietic cells as well as in developing BECs using differentiation of cultured ES cells. We identify ES cell–derived LECs as well as BECs and hematopoietic cells, and demonstrate that Tie2 signaling is essential for development of BECs and LECs, but not for hematopoietic cells.

Materials and methods

Cell preparation and culture conditions

TT2,[30] E14,[31] and R1[32] ES cells were maintained on mouse embryonic fibroblast (MEF) feeder cell layers in knockout Dulbecco-modified Eagle medium (Gibco BRL, Carlsbad, CA) containing 15% fetal bovine serum (Intergen, Purchase, NY), 100 U/mL leukemia inhibitory factor (LIF; Chemicon International, Temecula, CA), 0.1 mM nonessential amino acids (Gibco BRL), 1 mM sodium pyruvate (Gibco BRL), 2 mM L-glutamine (Gibco BRL), and 100 µM 2-mercaptoethanol (Sigma-Aldrich, St Louis, MO). After removal of LIF, ES cells were cultured on collagen type IV plates (Becton Dickinson, San Jose, CA) at 1×10^4 cells/mL for 2 days. Cells were then disaggregated by trypsin and seeded on OP9 cells at 1×10^5 cells/mL. After 5 days of culture, OP9 cells were removed from ES cells through a Sephadex G10 column (Amersham Bioscience, Uppsala, Sweden), and the ES cells were fractionated by Flk1 and Tie2 expression using FACSvantage (Becton Dickinson). Sorted cells were seeded on OP9 cells at 1000 to 15 000 cells/mL and cultured in the presence of VEGF-C (100 ng/mL; R&D Systems, Minneapolis, MN), VEGF-D (100 ng/mL; R&D Systems), or the caspase inhibitor Z-VAD-fmk (10-100 nM; Calbiochem, La Jolla, CA). When indicated, sorted cells were cultured with recombinant soluble Tie2-Fc fusion protein (30 µg/mL)[19] or recombinant soluble CD4-Fc fusion protein (30 µg/mL).[19]

Immunocytochemistry

Immunocytochemistry was performed essentially as described.[33] Differentiated ES cells cultured on OP9 cells were fixed with 4% paraformaldehyde at 4°C and stained with a rat monoclonal anti-mouse platelet–endothelial cell adhesion molecule 1 (PECAM-1) monoclona antibody (mAb) (MEC13.3; Becton Dickinson) or a rat monoclonal anti-mouse LYVE-1 antibody (ALY7[26]) by the indirect immunoperoxidase method using horseradish peroxidase–conjugated anti-rat IgG. Peroxidase activity was visualized using 3,3′-diaminobenzidine (Dojindo, Kumamoto, Japan). To determine whether Prox-1 was expressed in LYVE-1+ cells, we stained cells with biotinylated ALY7 and anti–Prox-1 antibody (Covance, Berkeley, CA). LYVE-1 and Prox-1 expression was detected by reacting with Alexa 488–conjugated Streptavidin (Molecular Probes, Eugene, OR) and Alexa 546–conjugated goat anti-rabbit antibody (Molecular Probes), respectively. For nuclear staining, cells were treated with TOTO3 (Molecular Probes). Stained cells were visualized by fluorescence microscopy. Stained and unstained cells were visualized by fluorescent microscopy (IX71) with either UplanApo 4×/0.13 NA, 10×/0.40 NA, or 20×/0.70 NA objectives (Olympus, Tokyo, Japan). Images were further processed with Adobe

Photoshop (Adobe Systems, San Jose, CA). For DiI labeling, 10 µg/mL DiI-Ac-LDL (Molecular Probes) was added to differentiated ES cells on OP9 cells and adherent cells were incubated for 4 hours at 37°C. After removing the media containing DiI-Ac-LDL, cells were washed and stained with anti–PECAM-1 (FITC-conjugated; Becton Dickinson) or anti–LYVE-1 (biotin-conjugated) plus FITC-conjugated Streptavidin (Becton Dickinson). Uptake of DiI-Ac-LDL by blood vessel endothelial cells (PECAM-1+ cells) and lymphatic endothelial cells (LYVE-1+ cells) was visualized using a standard rhodamine excitation emission filter (Olympus, Tokyo, Japan).

RT-PCR analysis

Total RNA was extracted from cells using RNeasy Kit (Qiagen, Hilder, Germany). Isolated RNA was reverse-transcribed using an reverse transcriptase (RT) for polymerase chain reaction (PCR) Kit (Clontech, Palo Alto, CA). cDNAs were amplified using Taq polymerase (TaKaRa, Kyoto, Japan). Sequences of gene-specific primers for RT-PCR were as follows: GATA2, 5′-(acacaccacccgatacccacctat), 3′-(cctacgccatggcagtcaccatgct); SCL, 5′-(cgcggatccacggagcggccgccgagcgcg), 3′-(cggaattccgcgccgcactactt-tggtgtg); c-myb, 5′-(gacagaagaggaggacagaatca), 3′-(tctcagggtcttcgtcgt-tatag); AML1, 5′-(ccagcaagctgaggagcggcg), 3′-(cggatttgtaaagacggtga); Tie2, 5′-(ttagttctctgtggagtcag), 3′-(aggccctgagttcttcactc); Flk1, 5′-(agaacac-caaaagagaggaacg), 3′-(gcacacaggcagaaaccagtag); VEGFR3, 5′-(gctaccact-gctactacaag), 3′-(gataatcccagtcgaaggtg); Prox1, 5′-(aagtggttcagcaatttccg), 3′-(tgaccttgtaaatggccttc); LYVE1, 5′-(ttcctcgcctctatttggac), 3′-(tctgttgtct-gcgtttcatcc); Pdpn, 5′-(gtgccagtgttgttctgggt), 3′-(tctgttgtctgcgtttcatcc); Evi1, 5′-(aatatgagtcatgccaaccc), 3′-(cttggtgtactgacatcatc); and GAPDH, 5′-(aatcccatcaccatcttcca), 3′-(ccaggggtcttactccttg).

PCR products were separated on a 1.2% agarose gel and gels were stained with ethidium bromide.

Quantitative RT-PCR analysis

Total RNA was isolated from 10^4 cells and cDNA was reverse-transcribed using Superscript III (Invitrogen, Carlsbad, CA) according to the manufacturer's instructions. The expression levels of Ang1, Ang2, and Ang3 were analyzed by quantitative (Q) RT-PCR using a LightCycler instrument (Roche Diagnostics, Mannheim, Germany) with LightCycler software version 3.5. cDNA was amplified for Q-PCR using SYBR Green 1 (Sigma-Aldrich) to detect PCR product. cDNA (2 µL) was used in a 20-µL final volume reaction containing 10 µL SYBR Premix Ex Taq (TaKaRa), 0.4 µM Ang1 forward (5′-GCCTTTGCACTAAAGAAGGTGTTTT-3′), and 0.4 µM Ang1 reverse (5′-ATACATCCGCACAGTCTCGAAATG-3′). The LightCycler was programmed to run an initial denaturation step at 95°C for 10 seconds followed by 45 cycles of denaturation (95°C for 5 seconds) and extension (60°C for 20 seconds), monitoring the synthesis of product at the end of the extension step of each cycle. The same conditions were used with primers Ang2 forward (5′-AGGAGATCAAGGCCTACTGT-GACA-3′) and Ang2 reverse (5′-GCTCCCGAA GCCCTCTTTG-3′), and Ang3 forward (5′-GTTCCAGGACTGTGCAGAGATCA-3′) and Ang3 reverse (5′-TCTCCATGTCACAGAACACCTTGAG-3′). The Ang1, Ang2, and Ang3 values were normalized against mouse β-actin (forward 5′-CAGCCTTCCTTCT-TGGGTATGG-3′; reverse 5′-CTGTGTTGGCATAGAGGTC TTTACG-3′).

Flow cytometric analysis and cell sorting

The following mAbs used for flow cytometry were purchased from Becton Dickinson: anti-CD34 (RAM34), anti-c-Kit (ACK45), anti-Sca-1 (E13-161.7), anti-CD45 (30-F11), anti-Flk1 (Avas12α1), anti-PECAM-1 (MEC13.3), anti-Mac-1 (M1/70), anti-Gr-1 (RB6-8C5), and anti-TER-119. Also used were anti-Tie2 mAb (TEK4)[34] and anti–LYVE-1 mAb (ALY7).[26] Fluorescence-activated cell sorting (FACS) analysis was performed on a FACSvantage (Becton Dickinson).

Progenitor assay by methylcellulose culture

Tie2+Flk1+ or Flk1+ cells derived from ES cells were embedded in 1 mL alpha medium containing 1.3% methylcellulose (1500 cp; Sigma-Aldrich), 30% fetal calf serum (FCS), 1% deionized bovine serum albumin (BSA;

Sigma-Aldrich). 0.1 mM 2-mercapto-ethanol (Sigma-Aldrich). 10 ng/mL stem cell factor (SCF: PeproTech EC. London. United Kingdom). 10 ng/mL recombinant mouse interleukin-3 (IL-3: PeproTech EC). 10 ng/mL recombinant human IL-6 (PeproTech EC). and 2 U/mL recombinant human erythropoietin (Epo: Chugai Pharmaceutical. Tokyo. Japan). Cells were cultured in a 35-mm culture dish and incubated at 37°C in a humidified atmosphere with 5% CO_2.

Statistics

Data are expressed as means plus or minus standard deviation (SD). Statistical analysis was conducted using the Student t test. Statistical significance was defined as a P value less than .05.

Results

In vitro differentiation of ES cells

In order to analyze the function of Tie2 in the development of LECs as well as BECs and hematopoietic cells, we developed a cell culture system for ES cell differentiation. After removal of LIF, E14 ES cells were cultured on collagen type IV plates for 2 days to initiate differentiation to a mesoderm lineage; subsequently, cells were transferred to OP9 stromal cells. Markers of both endothelial and hematopoietic cells, Sca-1, c-kit, and CD34, were expressed in undifferentiated ES cells (Figure 1A). Although 1% of ES cells expressed Flk1 on collagen plates, Tie2 was not expressed in Flk1 $^+$
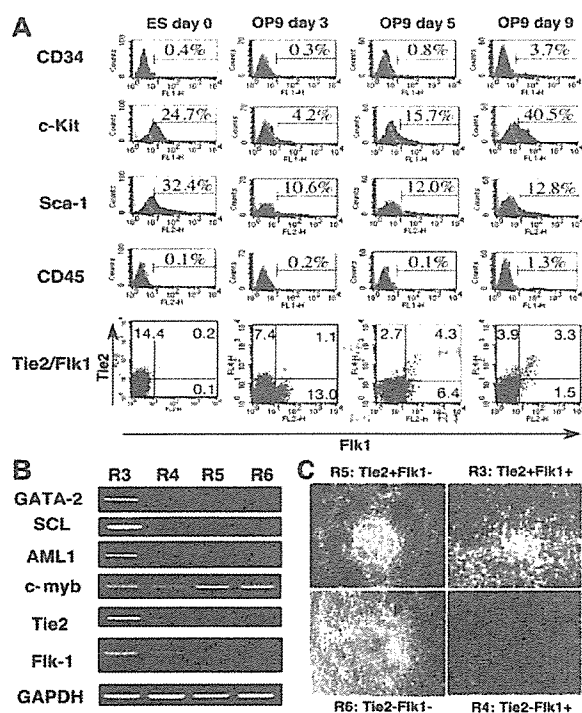

Figure 1. Mesodermal differentiation of ES cells on OP9 stromal cells. (A) E14 ES cells were cultured on collagen type IV plates for 2 days, and then all cells were cultured on OP9 cells for 9 days. The expression of CD34, c-Kit, Sca-1, CD45, Flk1, and Tie2 in ES cell–derived cells was analyzed at the indicated time points by flow cytometry. Stained $Tie^{-/-}$ cells are represented by purple shaded histograms. Unstained controls are represented by green lines. The percentages of cells in each quadrant are indicated. (B) Gene expression of fractionated cells shown in A (R3-R6) was analyzed by RT-PCR. (C) Fractionated cells (20 000; R3-R6) were cultured on OP9 cells. On day 7 of culture, hematopoietic clusters (red arrowheads) were developed only from the R3 fraction. In other fractions (R4-R6) hematopoietic clusters were not developed, but embryoid body–like colonies (blue arrowheads) developed from R5 and R6 fractions. Cells were analyzed at low (×40) magnification.

cells (data not shown). Following transfer of cells on collagen plates to OP9 cells, 8% of Flk1 $^+$ cells expressed Tie2 on day 3 of culture. Numbers of Tie2 $^+$ cells increased until day 5 of culture, when Tie2 expression was maximal; thereafter, both expression levels and numbers of Tie2 $^+$ cells gradually decreased. At day 9 of culture, cells cocultured with OP9 cells began expressing CD45, a marker of all hematopoietic cells except mature erythrocytes. Since Tie2 $^+$ cells appeared just before CD45 $^+$ hematopoietic cells, Tie2 $^+$ cells in the Flk1 $^+$ cell fraction may represent hematopoietic progenitor cells. We examined other ES strains, such as TT2 and R1 cells, using the same culture conditions, and confirmed that these strains showed a similar mesodermal phenotypes as E14 cells (data not shown).

Development of hematopoietic, lymphatic endothelial, and blood vessel endothelial cells from Flk1 $^+$Tie2 $^+$ cells

To analyze the differentiating potential of ES-derived cells, we fractionated cells on day 5 of culture using Tie2 and Flk1 mAb as shown in Figure 1A (bottom panel, R1-R4). Expression profiling of transcription factors specific for hematopoietic or endothelial cells was undertaken by RT-PCR (Figure 1B). Expression levels of GATA-2, SCL, and AML-1 in the Tie2 $^+$Flk1 $^+$ fraction (R3) were 1.7-, 2.5-, and 1.7-fold higher than those in the Tie2 $^-$Flk1 $^+$ fraction (R4), respectively. In the Flk1 $^-$ fraction (R5 and R6), expression levels of these genes were much lower compared with the Tie2 $^-$Flk1 $^+$ fraction (R4), suggesting that the Tie2 $^+$Flk1 $^+$ fraction may contain committed progenitors of hematopoietic and endothelial lineages. Cells (20 000) fractionated by Flk1 and Tie2 expression were cultured on OP9 cells (Figure 1C), and hematopoietic clusters formed only from the Tie2 $^+$Flk1 $^+$ fraction (R3) (Figure 1C, red arrowheads). Hematopoietic clusters were not detected in Flk1 $^+$Tie2 $^-$ (R4), Flk1 $^-$Tie2 $^+$ (R5), or Flk1 $^-$Tie2 $^-$ fractions (R6). The number of hematopoietic progenitors in each fraction was estimated by colony-forming assays in methylcellulose culture (Figure 2A-B). BECs were detected by staining with PECAM-1 mAb (Figure 2C). PECAM-1 $^+$ endothelial cells were spindle shaped and took up an acetyl-LDL (Figure 2D). To detect LECs, we generated a mAb against LYVE-1 (ALY7), a receptor for extracellular matrix glycosaminoglycan. Using this mAb, we detected LYVE-1 $^+$ cells on OP9 cells (Figure 2E). These cells also took up acetyl-LDL (Figure 2F), and 65% of them expressed Tie2 (Figure 2I). The lymphatic identity of these cells was further demonstrated by RT-PCR, using primers specific for LEC-enriched genes, namely, Pdpn, VEGFR3, and Prox1 (Figure 2J). Furthermore, LYVE-1 $^+$ cells coexpressed Prox-1 (Figure 2K). The presence of VEGFR-3 transcripts in these cultures provided the impetus for us to add the lymphatic growth factors, VEGF-C and VEGF-D. The addition of these factors resulted in a marked increase in the number of LYVE-1 $^+$ cells (Figure 2L) and an increase in the size of monolayers (VEGF-C, Figure 2G; VEGF-D, Figure 2H). These findings suggest that LYVE-1 $^+$ cells derived from ES cell differentiation cultures express many genes that are restricted to or enriched in LECs.

That Tie2 is required for these cell types is supported by the more than 10-fold increase in hematopoietic, blood vessel endothelial, and lymphatic endothelial colonies from Tie2+Flk1 $^+$ cells compared with Tie2 $^-$Flk1 $^+$ or Tie2 $^-$Flk1 $^-$ cell fractions (Table 1). To determine which cells produce the Tie2 ligands Ang1, Ang2, and Ang3 in order to support Tie2 $^+$ cells, we performed quantitative expression analysis for Ang1, Ang2, and Ang3. As shown in Figure 2M, OP9 cells and LYVE-1 $^-$ ES-derived cells expressed Ang1 but not Ang2 or Ang3. Although low expression levels of
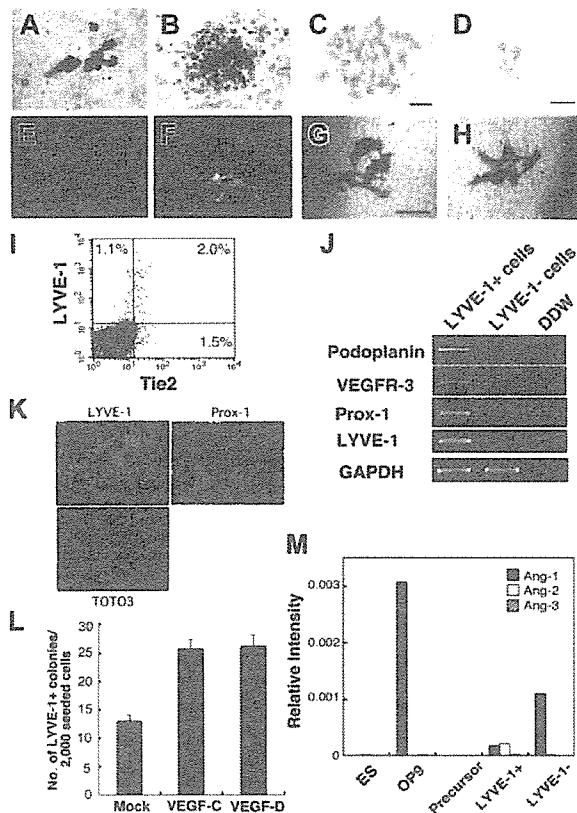
Figure 2. Development of lymphatic endothelial cells from ES cells. The Tie2⁺Flk1⁺ fraction of ES cell–derived cells formed erythroid colonies (A) and granulocyte-macrophage colonies (B) in methylcellulose. Vascular and lymphatic endothelial cells were stained with PECAM-1 mAb (C) and LYVE-1 mAb (D), respectively. PECAM-1⁺ cells (green, panel E) and LYVE-1⁺ cells (green, panel F) took up acetyl-LDL (red, panels E and F). Scale bars, 10 μm. (I) Expression of LYVE-1 and Tie2 in differentiated cells derived from ES cells on OP9 cells on day 6 of culture was analyzed by flow cytometry. The percentages of cells in each quadrant are indicated. (J) Lymphatic-specific genes, Pdpn, VEGFR-3, and Prox-1 in LYVE-1⁺ and LYVE-1⁻ cells were analyzed by RT-PCR. (K) Immunostaining at high magnification (× 200) showed that LYVE-1⁺ cells (green) coexpressed Prox-1 (red). TOTO3 (blue) was used to stain nuclei. (L) In the presence of VEGF-C and VEGF-D (100 ng/mL each), the number of LYVE-1⁺ colonies increased to 2 times that of mock-treated cells. Colonies were also larger in the presence of VEGF-C and VEGF-D (panels G and H, respectively). Results are expressed as the mean ± SD. (M) OP9 and ES cell–derived LYVE-1⁻ cells expressed Ang1. LYVE-1⁺ cells expressed low levels of Ang1 and Ang2. Ang1, Ang2, and Ang3 were not detectable in ES cells and lymphatic precursors (Flk1⁺ cells derived from ES cells).

Ang1 and Ang2 were detected in LYVE-1⁺ cells, ES cells and lymphatic precursor cells (ES cell–derived Flk1⁺ cells) did not express Ang's. These results suggest that Ang1 derived from OP9 cells might affect the growth or survival of Tie2⁺ cells.

Table 1. Frequency of hematopoietic and endothelial progenitors of differentiated ES cells

	Erythroid colonies from 30 000 cells	GM colonies from 30 000 cells	Vascular endothelial colonies from 1500 cells	Lymphatic endothelial colonies from 2000 cells
Tie2⁺Flk1⁺	11.3 ± 6.4	11.7 ± 2.1	47.5 ± 5.3	24.3 ± 2.5
Tie2⁻Flk1⁺	0	0	5.2 ± 1.8	0
Tie2⁺Flk1⁻	0	0	0	0
Tie2⁻Flk1⁻	0	0	0	0
Bulk	0	0	2.7 ± 1.5	1.3 ± 0.6

Development of hematopoietic and endothelial cells from Tie2-deficient ES cells

To clarify the function of Tie2 during hematopoietic and endothelial differentiation from ES cells, the differentiation capacity of $Tie2^{-/-}$ ES cells was examined using our culture system. $Tie2^{-/-}$ ES cells grew normally on MEF feeder layer cells (data not shown), and differentiated cells grown on OP9 cells were analyzed by flow cytometry. The frequency of cells expressing Flk1 in the $Tie2^{-/-}$ ES cells was similar to that seen in $Tie2^{+/-}$ cells (Figure 3A). RT-PCR of RNA from this fraction for expression of the genes involved in development of hematopoietic and endothelial cells revealed no remarkable differences between $Tie2^{+/-}$ and $Tie2^{-/-}$ cells (Figure 3B). To analyze hematopoietic development of $Tie2^{-/-}$ ES cells, we calculated the number of hematopoietic clusters formed on OP9 cells at day 7 of culture. The number and size of hematopoietic clusters of $Tie2^{-/-}$ ES cells were the same as those of $Tie2^{+/-}$ cells (Figure 3C, and data not shown). When the $Tie2^{-/-}$ hematopoietic clusters were transferred to fresh OP9 cells for an additional week, normal proliferating hematopoietic cells were detected by flow cytometry. Mature Mac-1–, Gr-1–, and Ter119–positive hematopoietic cells were differentiated from $Tie2^{-/-}$ ES cells (Figure 3D), and the frequency of mature hematopoietic cells was similar to that seen in $Tie2^{+/-}$ cells (data not shown), suggesting that Tie2 is not essential for development of hematopoietic cells. By contrast, $Tie2^{-/-}$ ES cells were severely defective in forming blood vessel and lymphatic endothelial colonies on OP9 cells at day 6 of culture. The number of such blood vessel and lymphatic endothelial colonies was approximately one
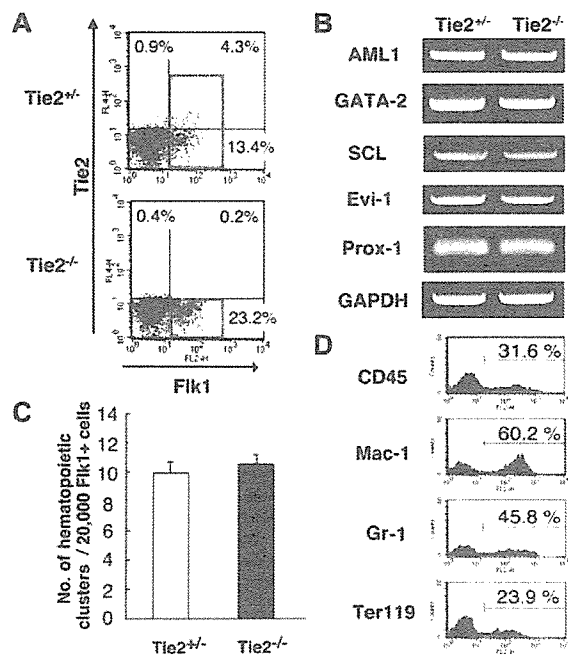

Figure 3. Normal development of hematopoietic cells from $Tie2^{-/-}$ ES cells. (A) FACS analysis of the expression of Flk1 and Tie2 in $Tie2^{-/-}$ and $Tie2^{+/-}$ ES cell–differentiated cells. Red squares show the Flk1⁺ fraction. The percentages of cells in each quadrant are indicated. (B) Expression of genes associated with mesoderm in Flk1⁺ cells shown in panel A (red squares) was analyzed by RT-PCR. (C) Flk1⁺ cells (20 000) were cultured on OP9 cells. The number of hematopoietic clusters from $Tie2^{+/-}$ and $Tie2^{-/-}$ cells at day 7 of culture was calculated. Results are expressed as the mean ± SD. (D) $Tie2^{-/-}$ hematopoietic clusters were cultured for an additional 7 days on fresh OP9 cells. The expression of CD45, Mac-1, Gr-1, and Ter119 was analyzed by flow cytometry. ES cell–derived hematopoietic cells are represented by purple shaded histograms; unstained controls, by green lines.
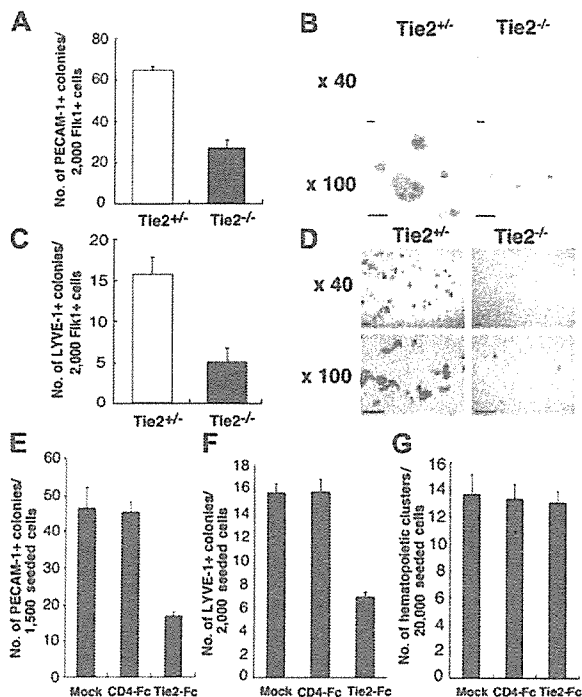
Figure 4. Lymphatic and blood vessel endothelial cell development from Tie2$^{-/-}$ ES cells. (A) Flk1$^+$ cells (2000) were cultured on OP9 cells. At day 7 of culture, the number of vascular endothelial colonies developed from Tie2$^{+/-}$ (□) and Tie2$^{-/-}$ (■) ES cells was calculated. (B) Vascular endothelial colonies were stained with PECAM-1 mAb and analyzed at low (× 40) and high (× 100) magnification. (C) The number of lymphatic endothelial colonies developed from Tie2$^{+/-}$ (□) and Tie2$^{-/-}$ (■) ES cells was calculated. (D) Lymphatic endothelial colonies were stained with LYVE-1 mAb and analyzed at low (× 40) and high (× 100) magnification. Scale bars in panels B and D, 20 μm. In the presence of Tie2-Fc (30 μg/mL), the number of vascular and lymphatic endothelial colonies was decreased (panels E and F, respectively). (G) Hematopoietic cluster formation was not affected by exogenous soluble Tie2-Fc (30 μg/mL). Exogenous soluble CD4-Fc (30 μg/mL) served as the control. Results in panels A, C, and E-G are expressed as the mean ± SD.

third that observed from Tie2$^{+/-}$ cells (Figure 4A-B), and colony size was smaller than that seen from Tie2$^{+/-}$ cells (Figure 4C-D). These results suggest that Tie2 function is required for development of BECs and LECs, but not of hematopoietic cells. To confirm these findings, we added soluble Tie2-Fc fusion protein to the culture media of wild-type ES cells to block Tie2 signaling. As shown in Figure 4E-G, the number of vascular and lymphatic endothelial cell colonies derived from wild-type ES cells in the presence of soluble Tie2-Fc fusion protein decreased to one half to one third of the mock-treated cells, while the number of hematopoietic clusters was not affected by soluble Tie2-Fc fusion protein. We did not detect such inhibition in the presence of soluble CD4-Fc fusion protein (Figure 4 E-F).

Tie2 signaling is crucial for antiapoptotic signaling in the development of lymphatic and blood vessel endothelial cells

To further analyze the mechanisms underlying defective proliferation of BECs and LECs from Tie2$^{-/-}$ ES cells, we analyzed expression of blood vessel– and lymphatic-specific markers PECAM-1 and LYVE-1, respectively, by flow cytometry at days 2, 4, and 6 of culture (Figure 5A). Cells expressing PECAM-1 and LYVE-1 in Tie2$^{-/-}$ ES cells decreased over 6 days. PECAM-1$^+$ cells in Tie2$^{-/-}$ cells were approximately one third the number of those in Tie2$^{+/-}$ cells at day 6 of culture, as was the case with LYVE-1$^+$ cells (Figure 5B-C). This finding suggested that Tie2$^{-/-}$-mediated signaling

protects endothelial cells from cell death. To test this possibility, we treated Tie2$^{-/-}$ cells with the caspase inhibitor Z-VAD-fmk. As shown in Figure 5B and C, lymphatic and blood vessel endothelial colony formation was rescued in the presence of Z-VAD-fmk in a dose-dependent fashion. In the presence of 50 nM of Z-VAD-fmk, the number of lymphatic endothelial colonies from Tie2$^{-/-}$ cells was rescued to 60% of that from Tie2$^{+/-}$ cells (Figure 5C), although the size of Tie2$^{-/-}$ lymphatic endothelial colonies remained small (Figure 5D). The formation of blood vessel endothelial colonies was similar in the presence of Z-VAD-fmk (50 nM; Figure 5C). These findings suggest that Tie2 signaling is crucial for LEC and BEC development and mediates antiapoptotic signaling during ES cell differentiation.

Discussion

Although we have demonstrated that Tie2 is expressed in the vitelline artery,[19] the AGM region,[4] and fetal liver,[20] the function of Tie2 in development has not been elucidated. The early death of Tie2$^{-/-}$ embryos precludes detailed analysis of the role of Tie2 in
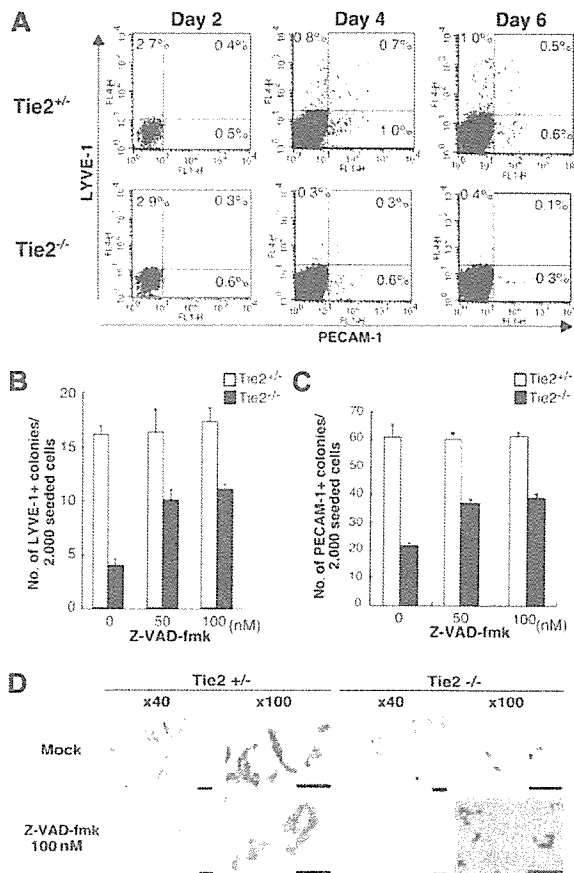

Figure 5. Tie2 signaling in blood vessels and lymphatic endothelial cells protected from apoptosis. (A) Expression of PECAM-1 and LYVE-1 in ES cell–derived cells was analyzed by flow cytometry at days 2, 4, and 6 of culture. The percentages of cells in each quadrant are indicated. (B) Addition of the caspase inhibitor Z-VAD-fmk (50 nM) to the culture media rescued the number of LYVE-1$^+$ colonies from Tie2$^{-/-}$ ES cells (■). (C) The number of PECAM-1$^+$ colonies from Tie2$^{-/-}$ ES cells (■) was also rescued in the presence of Z-VAD-fmk (50 nM). Results are expressed as mean ± SD. (D) In the presence of Z-VAD-fmk, the size of Tie2$^{-/-}$ lymphatic endothelial cells was unchanged, although the number of lymphatic colonies was partially rescued. Scale bars, 20 μm.

development of hematopoietic and endothelial lineages. Using an ES cell differentiation system, we have analyzed the development of hematopoietic cells as well as BECs and LECs from $Tie2^{-/-}$ ES cells. At day 8 of culture on OP9 cells, the normal formation of hematopoietic clusters from $Tie2^{-/-}$ cells suggests that Tie2 signaling does not contribute to development of hematopoietic cells from precursors. Furthermore, differentiation of myeloid cells from $Tie2^{-/-}$ hematopoietic clusters was normal. These results indicate that Tie2 is not essential for development of hematopoietic cells from ES cells. Recently, Puri and Bernstein[21] used combined mosaic analysis to demonstrate that Tie receptors are not required for differentiation and proliferation of definitive hematopoietic lineages in the embryo and fetus. Their findings are consistent with what we show in this study. Although our in vitro differentiation experiments suggest that Tie2 is not essential for hematopoiesis during development, Ang1/Tie2 signaling in hematopoietic cells has been reported to function to maintain hematopoietic stem cells in the bone marrow niche where Ang1 is expressed by osteoblasts.[18] Thus Tie2 function in hematopoiesis would seem to be specific for adult bone marrow.

Although much is known about normal and pathologic development of the vascular system,[35] the lack of specific markers has made it difficult to follow the development of the lymphatic system. In order to identify LECs, we recently generated a LEC-specific mAb against LYVE-1.[26] This mAb allowed us to detect LECs in mouse embryos at midgestation and purify these cells. ES cell–derived LYVE-1$^+$ cells express LEC-specific genes, such as *Prox1*, *Pdpn*, and *VEGFR3*, and exhibit DiI-Ac-LDL uptake. Furthermore, VEGF-C and VEGF-D, lymphatic growth factors, increased the number of LYVE-1–positive endothelial colonies from ES cells. These findings indicate that LYVE-1$^+$ cells isolated from these cultures have many characteristics of LECs. Lymphatic vasculature of the thoracic and abdominal viscera have been proposed to arise by endothelial spreading from lymph sacs.[6,36] This proposal is supported by the finding that budding of endothelial cells from the veins of Prox-1 mutant embryos is arrested.[9,10] To clarify the mechanisms of lymphangiogenesis in vitro, we analyzed the function of Tie2. In this study LECs were differentiated from ES cell–derived Tie2$^+$Flk1$^+$ cells, and approximately 1% of Tie2$^+$Flk1$^+$ cells formed lymphatic endothelial colonies on OP9 cells. Our in vitro differentiation assay allows us to clarify the mechanisms of LEC development from its precursor.

Thus far, Tie2 signaling has been reported to be required for proper development and function of the vascular system. Mice lacking Ang2 exhibit lymphatic vessel defects, strongly suggesting a role of Tie2 signaling in lymphangiogenesis.[37] In this study we have shown that LECs and BECs can be differentiated from Tie2$^+$Flk1$^+$ cells, and that 65% of LYVE-1$^+$ LECs express Tie2. To analyze the function of Tie2 in the development of lymphatic

endothelial cells, we performed FACS analysis and immunocytochemistry during differentiation of $Tie2^{-/-}$ ES cells. FACS analysis revealed that $Tie2^{-/-}$ cells expressing LYVE-1 decreased over time as did PECAM-1$^+$ BECs. Treatment with a caspase inhibitor, which specifically inhibits apoptosis, partially rescued defective formation of lymphatic and blood vessel endothelial colonies from $Tie2^{-/-}$ cells, suggesting that both endothelial cells undergo apoptosis in the absence of Tie2 signaling. Although Tie2 signaling contributed to the survival of both LECs and BECs on OP9 cells, treatment with the caspase inhibitor did not affect the size of $Tie2^{-/-}$ colonies. Based on these findings, we propose that Tie2 cooperates with other signaling pathways involved in growth. Although we do not identify these pathways, OP9 cells are known to secrete several growth factors, including VEGF-C and VEGF-D.[38] FACS analysis also revealed that at day 2 of culture, the frequency of LYVE-1$^+$ and PECAM-1$^+$ cells derived from $Tie2^{-/-}$ cells was comparable with frequencies seen in $Tie2^{+/-}$ cells, suggesting that lymphatic and blood vessel endothelial precursors develop normally from $Tie2^{-/-}$ cells. A gene expression study clearly showed that expression levels of Prox-1 in lymphatic precursors (the Flk1$^+$ cell fraction) of $Tie2^{-/-}$ cells were comparable with those seen in $Tie2^{+/-}$ cells, suggesting that Tie2 deficiency does not affect Prox-1 expression. These findings suggest that Tie2 is not essential for development of lymphatic and blood vessel endothelial precursors, although both types of endothelial cells from $Tie2^{-/-}$ cells undergo apoptosis due to lack of Tie2 signaling.

Regarding vascular endothelial cells, in vivo study has shown that mice lacking Ang1 and Tie2 develop a fairly normal primary vasculature, but that this vasculature fails to undergo further normal remodeling.[28,39,40] We have demonstrated that lymphatic endothelial cells express Tie2 in both embryonic and adult settings, and that the activation of Tie2 signaling by Ang1 stimulates both in vivo lymphatic angiogenesis in mouse cornea and in vitro colony formation of lymphatic endothelial cells.[26] Data from both in vitro ES cell differentiation and in vivo embryonic development suggest that Ang/Tie2 signaling may contribute to regulation of lymphatic vessel formation in the development of lymphatic vessels.

In summary, our results derived from induction studies of ES cells have revealed that Tie2 is expressed in the precursors of mesodermal lineages, hematopoietic cells, and endothelial cells. We have also shown that Tie2 is not essential for development of hematopoietic cells, but that it plays an important role in antiapoptotic signaling in lymphatic and blood vessel development.

Acknowledgment

References

1. Sabin F. Studies on the origin of blood vessels and red corpuscles as seen in the living blastoderm of the chick during the second day of incubation. Contribut Embryol. 1920;9:213-262.

2. Kubo H, Alitalo K. The bloody fate of endothelial stem cells. Genes Dev. 2003;17:322-329.

3. Haar JL, Ackerman GA. A phase and electron microscopic study of vasculogenesis and erythropoiesis in the yolk sac of the mouse. Anat Rec. 1971;170:199-223.

4. Hamaguchi I, Huang XL, Takakura N, et al In vitro hematopoietic and endothelial cell development from cells expressing TEK receptor in murine

aorta-gonad-mesonephros region. Blood. 1999; 93:1549-1556.

5. Choi K, Kennedy M, Kazarov A, Papadimitriou JC, Keller G. A common precursor for hematopoietic and endothelial cells. Development. 1998; 125:725-732.

6. Sabin FR. On the origin of the lymphatic system from the veins, and the development of the lymph hearts and thoracic duct in the pig. Am J Anat. 1902;1:367-389.

7. Oliver G, Detmar M. The rediscovery of the lymphatic system: old and new insights into the development and biological function of the lymphatic vasculature. Genes Dev. 2002;16:773-783.

8. Jeltsch M, Kaipainen A, Joukov V, et al. Hyperplasia of lymphatic vessels in VEGF-C transgenic mice. Science. 1997;276:1423-1425.

9. Wigle JT, Oliver G. Prox1 function is required for the development of the murine lymphatic system. Cell. 1999;98:769-778.

10. Wigle JT, Harvey N, Detmar M, et al. An essential role for Prox1 in the induction of the lymphatic endothelial cell phenotype. EMBO J. 2002;21: 1505-1513.

11. Shalaby F, Rossant J, Yamaguchi TP, et al. Failure of blood-island formation and vasculogenesis in Flk-1-deficient mice. Nature. 1995;376:62-66.

12. Shalaby F, Ho J, Stanford WL, et al. A requirement for Flk1 in primitive and definitive hematopoiesis and vasculogenesis. Cell. 1997;89:981-990.

13. Millauer B, Wizigmann-Voos S, Schnurch H, et al. High affinity VEGF binding and developmental expression suggest Flk-1 as a major regulator of vasculogenesis and angiogenesis. Cell. 1993;72:835-846.

14. Dumont DJ, Fong GH, Puri MC, Gradwohl G, Alitalo K, Breitman ML. Vascularization of the mouse embryo: a study of flk-1, tek, tie, and vascular endothelial growth factor expression during development. Dev Dyn. 1995;203:80-92.

15. de Vries C, Escobedo JA, Ueno H, Houck K, Ferrara N, Williams LT. The fms-like tyrosine kinase, a receptor for vascular endothelial growth factor. Science. 1992;255:989-991.

16. Dumont DJ, Gradwohl GJ, Fong GH, Auerbach R, Breitman ML. The endothelial-specific receptor tyrosine kinase, tek, is a member of a new subfamily of receptors. Oncogene. 1993;8:1293-1301.

17. Iwama A, Hamaguchi I, Hashiyama M, Murayama Y, Yasunaga K, Suda T. Molecular cloning and characterization of mouse TIE and TEK receptor tyrosine kinase genes and their expression in hematopoietic stem cells. Biochem Biophys Res Commun. 1993;195:301-309.

18. Arai F, Hirao A, Ohmura M, et al. Tie2/angiopoietin-1 signaling regulates hematopoietic stem cell quiescence in the bone marrow niche. Cell. 2004;118:149-161.

19. Takakura N, Huang XL, Naruse T, et al. Critical role of the TIE2 endothelial cell receptor in the development of definitive hematopoiesis. Immunity. 1998;9:677-686.

20. Hsu HC, Ema H, Osawa M, Nakamura Y, Suda T, Nakauchi H. Hematopoietic stem cells express Tie-2 receptor in the murine fetal liver. Blood. 2000;96:3757-3762.

21. Puri MC, Bernstein A. Requirement for the TIE family of receptor tyrosine kinases in adult but not fetal hematopoiesis. Proc Natl Acad Sci U S A. 2003;100:12753-12758.

22. Koblizek TI, Weiss C, Yancopoulos GD, Deutsch U, Risau W. Angiopoietin-1 induces sprouting angiogenesis in vitro. Curr Biol. 1998;8:529-532.

23. Papapetropoulos A, Garcia-Cardena G, Dengler TJ, Maisonpierre PC, Yancopoulos GD, Sessa WC. Direct actions of angiopoietin-1 on human endothelium: evidence for network stabilization, cell survival, and interaction with other angiogenic growth factors. Lab Invest. 1999;79:213-223.

24. Kwak HJ, So JN, Lee SJ, Kim I, Koh GY. Angiopoietin-1 is an apoptosis survival factor for endothelial cells. FEBS Lett. 1999;448:249-253.

25. Jones N, Voskas D, Master Z, Sarao R, Jones J, Dumont DJ. Rescue of the early vascular defects in Tek/Tie2 null mice reveals an essential survival function. EMBO Rep. 2001;2:438-445.

26. Morisada T, Oike Y, Yamada Y, et al. Angiopoietin-1 promotes LYVE-1-positive lymphatic vessel formation. Blood. 2005;105:4649-4656.

27. Tammela T, Saaristo A, Lohela M, et al. Angiopoietin-1 promotes lymphatic sprouting and hyperplasia. Blood. 2005;105:4624-4648.

28. Dumont DJ, Gradwohl G, Fong GH, et al Dominant-negative and targeted null mutations in the endothelial receptor tyrosine kinase, tek, reveal a critical role in vasculogenesis of the embryo. Genes Dev. 1994;8:1897-1909.

29. Puri MC, Rossant J, Alitalo K, Bernstein A, Partanen J. The receptor tyrosine kinase TIE is required for integrity and survival of vascular endothelial cells. EMBO J. 1995;14:5884-5891.

30. Yagi T, Tokunaga T, Furuta Y, et al. A novel ES cell line, TT2, with high germline-differentiating potency. Anal Biochem. 1993;214:70-76.

31. Hooper M, Hardy K, Handyside A, Hunter S, Monk M. HPRT-deficient (Lesch-Nyhan) mouse embryos derived from germline colonization by cultured cells. Nature. 1987;326:292-295.

32. Nagy A, Rossant J, Nagy R, Abramow-Newerly W, Roder JC. Derivation of completely cell culture-derived mice from early-passage embryonic stem cells. Proc Natl Acad Sci U S A. 1993;90:8424-8428.

33. Takakura N, Yoshida H, Ogura Y, Kataoka H, Nishikawa S. PDGFR alpha expression during mouse embryogenesis: immunolocalization analyzed by whole-mount immunohistostaining using the monoclonal anti-mouse PDGFR alpha antibody APA5. J Histochem Cytochem. 1997;45:883-893.

34. Yano M, Iwama A, Nishio H, Suda J, Takada G, Suda T. Expression and function of murine receptor tyrosine kinases, TIE and TEK, in hematopoietic stem cells. Blood. 1997;89:4317-4326.

35. Gale NW, Yancopoulos GD. Growth factors acting via endothelial cell-specific receptor tyrosine kinases: VEGFs, angiopoietins, and ephrins in vascular development. Genes Dev. 1999;13:1055-1066.

36. Gray H. In Anatomy of the human body. In: Clemente CD, ed. The Lymphatic System. Philadelphia, PA: Lea and Febiger; 1985:866-932.

37. Gale NW, Thurston G, Hackett SF, et al. Angiopoietin-2 is required for postnatal angiogenesis and lymphatic patterning, and only the latter role is rescued by Angiopoietin-1. Dev Cell. 2002;3:411-423.

38. Matsumura K, Hirashima M, Ogawa M, et al. Modulation of VEGFR-2-mediated endothelial-cell activity by VEGF-C/VEGFR-3. Blood. 2003;101:1367-1374.

39. Suri C, Jones PF, Patan S, et al. Requisite role of angiopoietin-1, a ligand for the TIE2 receptor, during embryonic angiogenesis. Cell. 1996;87:1171-1180.

40. Sato TN, Tozawa Y, Deutsch U, et al. Distinct roles of the receptor tyrosine kinases Tie-1 and Tie-2 in blood vessel formation. Nature. 1995;376:70-74.

Morphological identification of hepatitis C virus E1 and E2 envelope glycoproteins on the virion surface using immunogold electron microscopy

MASAHIKO KAITO[1], SHOZO WATANABE[2], HIDEAKI TANAKA[1], NAOKI FUJITA[1], MASAYOSHI KONISHI[1], MOTOH IWASA[1], YOSHINAO KOBAYASHI[1], ESTEBAN CESAR GABAZZA[1], YUKIHIKO ADACHI[1], KYOKO TSUKIYAMA-KOHARA[3] and MICHINORI KOHARA[3]

[1]Department of Gastroenterology and Hepatology, Division of Clinical Medicine and Biomedical Science, Institute of Medical Science, Mie University Graduate School of Medicine, 2-174 Edobashi, [2]Health Administration Center, Mie University, 1577 Kurimamachiya-cho, Tsu, Mie 514-8507; [3]Department of Microbiology of Cell Biology, Tokyo Metropolitan Institute of Medical Science, 3-18-22, Honkomagome, Bunkyo-ku, Tokyo 113-8613, Japan

Abstract. It is known that hepatitis C virus (HCV) particles are spherical, 55-65 nm particles with fine surface projections of about 6 nm in length and with a 30-35 nm inner core. We have reported that free HCV particles labeled with gold particles specific to the HCV E1 glycoprotein are located in 1.14-1.16 g/ml fractions from plasma samples with high HCV RNA titers after sucrose density gradient centrifugation. However, the morphology of the HCV E2 glycoprotein on the virion has not yet been elucidated. To visualize HCV E2 localization on the virion, we used the same plasma samples where HCV particles were clearly shown. An indirect immunogold electron microscopic study was carried out using monoclonal and polyclonal anti-HCV E2 antibodies. HCV-like particles specifically reacted with the anti-HCV E2 antibodies. Moreover, to evaluate the localization of the HCV E1 and E2 glycoproteins on the virion surface, an immunogold electron microscopic study using double labeling with anti-HCV E1 antibodies and anti-HCV E2 antibodies was also performed. These particles also specifically reacted with both anti-E1 and E2 antibodies. This is the first report showing the presence of both HCV E1 and E2 glycoproteins on HCV virion surface in human plasma samples.

Introduction

Hepatitis C virus (HCV) is the main causative agent of non-A non-B hepatitis. It is estimated that 170 million individuals are infected with HCV worldwide (1). HCV is a hepatotropic, enveloped RNA virus that belongs to the genus *Hepacivirus* of the *Flaviviridae* family (2), and it is the leading cause of acute hepatitis, chronic hepatitis, liver cirrhosis and hepatocellular carcinoma in humans (1,3-6). The HCV genome is a positive-stranded RNA of 9.6 kb containing a single open reading frame and two untranslated regions (7-9). It encodes a polyprotein of 3010 amino acids, which is cleaved into single proteins by a host signal peptidase in the structural region and by HCV-encoded proteases in the nonstructural region. Structural components include the capsid protein and the envelope glycoproteins E1 and E2. The nonstructural components include NS2, NS3, NS4A, NS4B, NS5A and NS5B. The NS2, NS3, and NS 4A proteins function as proteases, the NS3 protein as helicase, and the NS5B protein as RNA-dependent RNA polymerase (1).

HCV E1 and E2 glycoproteins are possible virion envelope glycoproteins, and their molecular weights are 35 and 70 kDa, respectively (10,11). The comparison of HCV genome structure with flaviviruses suggests that HCV E1 (gp35) and E2 (gp70) glycoproteins interact forming heterodimer complexes as the basic subunit of the HCV virion envelope (11,12). However, this has not been confirmed morphologically. We previously demonstrated that HCV particles are spherical, 55-65 nm particles with fine surface projections of about 6 nm in length and with a 30-35 nm inner core by immunoelectron microscopic study using anti-HCV E1 antibodies (13-17). Free HCV particles were found in 1.14-1.16 g/ml fractions after sucrose density gradient

Correspondence to: Dr Masahiko Kaito, Department of Gastroenterology and Hepatology, Division of Clinical Medicine and Biomedical Science, Institute of Medical Science, Mie University Graduate School of Medicine, 2-174 Edobashi, Tsu, Mie 514-8507, Japan
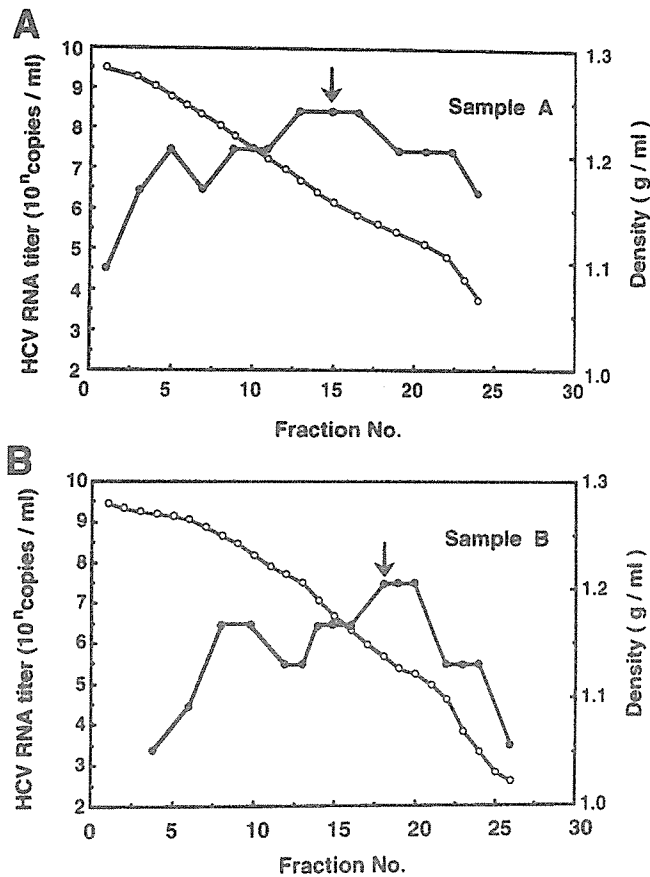E-mail: kaitoma@clin.medic.mie-u.ac.jp

Figure 1. HCV-RNA titers in fractions from samples A and B obtained by sucrose density gradient centrifugation. HCV RNA titers (●) and buoyant densities (o) are shown: (A) sample A, (B) sample B. Arrows indicate the fractions (1.14-1.16 g/ml) in which HCV particles were successfully detected by immunogold EM using rabbit anti-HCV E1 polyclonal antibody (RR2).

centrifugation. However, the morphology of the HCV E2 glycoprotein on the virion has not as yet been elucidated.

In this study, we carried out indirect immunogold electron microscopy (EM) in order to evaluate the localization of the HCV E1 and E2 glycoproteins on the surface of HCV particles isolated from plasma samples with high HCV RNA titers.

Materials and methods

Virus samples. Plasma samples where HCV particles were clearly shown, were used to determine the HCV E2 localization on HCV particles. HCV particle isolation and indirect immunogold EM were performed as previously described (13). In brief, virus samples from HCV RNA-rich plasma sample A [alanine aminotransferase (ALT): 10^3 IU/l, HCV RNA: genotype 1b (18), 4×10^7 copies/ml] and B (ALT: 10^9 IU/l, genotype 1b, 5×10^7 copies/ml), and anti-HCV-negative plasma sample C (ALT: 121 IU/l) and D (ALT: 87 IU/l) were prepared as follows: 100 ml of plasma were centrifuged at 75000 g for 6 h at 4°C and the suspension of the pellet was centrifuged again at 150000 g for 2.5 h at 4°C. A 1000-fold concentrated suspension of the sample was layered on a 20-60% (w/w) continuous sucrose density gradient in TNE buffer (50 mM Tris-HCl, pH 7.5, 100 mM

NaCl, 1 mM EDTA), and centrifuged at 100000 g for 16 h at 4°C. Sucrose fractions (500 μl) were collected from the tube bottom, and the sucrose densities were measured with an Abbé refractometer. The distribution of HCV RNA titers was determined using competitive polymerase chain reaction (PCR) (19,20). HCV RNA titers in fractions from samples A and B obtained by sucrose density gradient centrifugation were previously described (13,17). The density at which the highest HCV RNA titers (sample A, 5×10^8 copies/ml; sample B, 5×10^7 copies/ml) were found was 1.14-1.17 g/ml for sample A and 1.12-1.14 g/ml for sample B (Fig. 1). For preparing a 1000-fold concentrated virus sample, each sucrose fraction was diluted in 12 ml of PBS (pH 7.4), and spun down at 150000 g for 2.5 h at 4°C. The pellets were then suspended in 100 μl of PBS. The fractions (1.14-1.16 g/ml) in which HCV particles were successfully detected by immunogold EM using rabbit anti-HCV E1 polyclonal antibody (13) were used for virus sampling.

Rabbit polyclonal and mouse monoclonal antibodies to HCV E2 glycoprotein. The rabbit polyclonal anti-HCV E2 antibody (RR6) was prepared and characterized as follows. The putative E2 gene of HCV genotype 1b (nucleotide position 1068-2430) (8,10) was cloned under the control of the ATL-P7.5 hybrid promoter of the vaccinia virus vector pSFB4 (21), and allowed to recombine with the Liter strain of vaccinia virus to give a vector recombinant vaccinia virus (RVV). Rabbits were infected intradermally with 10^8 p.f.u. of RVV and 2 months later were boosted twice with the purified putative E2 glyco-protein. Putative HCV E2 glycoprotein was expressed by RVV and purified by lentil lectin column chromatography and affinity chromatography using an anti-E2 monoclonal antibody. Mouse monoclonal antibodies (747, 843, 1518, 1671, and 1864) against the putative HCV [genotype 1b (17)] E2 glycoprotein were prepared by immunization of mice with purified recombinant E2 glycoprotein (gp70) expressed by RVV. The antibody RR6 and the monoclonal antibodies were screened by enzyme-linked immunosorbent assay (ELISA) using synthetic peptides and purified recombinant protein, indirect immunofluorescence assay (IFA) using RVV- and baculovirus-infected (22) rabbit kidney cells, and Western blot analysis (WB) using purified E2 protein region of HCV genotype 1b as antigens (8). The epitope of mono-clonal antibodies was mapped using residues of 20 synthetic peptides whose adjacent peptides overlap by 10 amino acids corresponding to the amino acid sequence reported by Kato *et al* (7). The characteristics of anti-HCV E2 antibodies used as the primary antibody of the indirect immunogold reaction were determined (Table I). The antibody RR6 and the mono-clonal antibodies reacted specifically with the putative HCV E2 glycoprotein, but it did not react with the putative HCV core, E1, or NS2 proteins. Specificity was determined by using primary antibodies from pre-immune normal rabbit serum, serum from a rabbit infected with the Lister strain of vaccinia virus and monoclonal antibody specific to human blood type A antigen as negative controls, or by omitting the use of the primary antibody.

Rabbit polyclonal and mouse monoclonal antibodies to HCV E1 glycoprotein. The rabbit polyclonal antibody (RR2) and

Table I. Characteristics of polyclonal and monoclonal antibodies to the putative HCV E2 glycoprotein.

Antibody	ELISA[a] titer	IFA[b] titer	WB[c] titer	Epitope[d] (amino acid position)[e]
Polyclonal				
RR6	10^6	$\geq 10^3$	$\geq 10^3$	
Monoclonal				
747	<0.1 μg/ml	<10 μg/ml	< 1 μg/ml	520-540
843	<0.1 μg/ml	<10 μg/m	<10 μg/ml	520-540
1518	<0.1 μg/ml	<10 μg/ml	<10 μg/ml	450-470
1671	<0.1 μg/ml	<10 μg/ml	<10 μg/ml	640-660
1864	<0.1 μg/ml	<0 μg/ml	<1 μg/ml	450-470

[a]Carried out using synthetic peptides and purified recombinant HCV E2 glycoproteins. [b]Performed using recombinant vaccinia virus- and baculovirus-infected cells. [c]Western blot analysis, using purified recombinant glycoproteins from the putative E2 glycoprotein region of HCV genotype 1b. [d]Mapped using 20-amino acid oligopeptides, each overlapping the adjacent oligopeptide by 10 amino acids. [e]Kato et al (7).

mouse monoclonal antibodies (159, 260, 305 and 1905) to the HCV E1 glycoprotein were described previously (13).

Electron microscopy and immunogold electron microscopy. For conventional EM, 3 μl of each virus sample was applied to formvar-coated and carbon-vaporized grids and then negatively stained with 2% phosphotungstic acid, pH 6.5. The grid was examined under a Hitachi H-800 electron microscope operated at 100 kV. Indirect immunogold EM was performed as previously described (13-17). In brief, 3 μl of each virus sample was adsorbed on the grid and then the semidried grid was floated for 5 min on a drop of TBS-BSA (100 mM Tris-HCl, pH 7.6, 150 mM NaCl, and 2% bovine serum albumin) placed on parafilm in a moist chamber. The grid was then floated for 30 min on a drop of TBS containing 3% gelatin and then the excess gelatin from the drop of TBS-BSA was washed away. The grid was incubated for 60 min on a drop of primary antibody solution (diluted 1:100 in TBS-BSA) at room temperature, and then washed three times with TBS-BSA. After incubating the grid for 60 min in a drop of secondary antibody solution (diluted 1:20 in TBS-BSA), the grid was washed three times with TBS-BSA and once with TBS. The grid was negatively stained with 2% phosphotungstic acid for EM observation. Indirect immunogold EM was performed using rabbit anti-HCV E2 antibody RR6 at a dilution of 1:100 or a mixture of five monoclonal anti-HCV E2 antibodies (747, 843, 1518, 1671 and 1864), at a dilution of 1:10 as a primary antibody, and goat anti-rabbit IgG colloidal gold particles (10 nm in diameter; BioCell Research Laboratories, Cardiff, UK) or staphylococcal Protein A-conjugated colloidal gold particles (5 nm in diameter, BioCell Research Laboratories) as a secondary antibody. HCV particles (genotype 1b, 10^8 copies/ml of HCV RNA) in 1.14-1.16 g/ml sucrose fractions were incubated on carbon-coated copper grids with RR6 at a dilution of 1:100 and with a mixture of five clones of mouse anti-HCV E2 monoclonal antibodies at a dilution of 1:10. The HCV E1 and E2 glycoproteins on the virion were double labeled as follows. HCV particles were initially incubated with a mixture of four

clones of mouse anti-HCV E1 monoclonal antibodies (159, 260, 305 and 1905) at a dilution of 1:10 and protein A-conjugated 5 nm-gold particles at a dilution of 1:20. Then, the sample was treated with rabbit anti-HCV E2 polyclonal antibody (RR6) at a dilution of 1:100 and with goat anti-rabbit IgG-conjugated 10 nm-gold particles at a dilution of 1:20. Finally, the samples were stained with 2% phosphotungstic acid for EM observation. In addition, HCV particles were initially incubated with a mixture of five clones of mouse anti-HCV E2 monoclonal antibodies (747, 843, 1518, 1671, and 1864) at a dilution of 1:10 and protein A-conjugated 5 nm-gold particles at a dilution of 1:20, and then reacted with the rabbit anti-HCV E1 polyclonal antibody (RR2) at a dilution of 1:100 and with goat anti-rabbit IgG-conjugated 10 nm-gold particles at a dilution of 1:20. Finally, the samples were stained with 2% phosphotungstic acid.

Results

Localization of the HCV E2 glycoprotein on the surface of the virion. HCV-like particles (55-65 nm) with fine 6 nm spikes were visualized in sucrose fractions at a density of 1.14-1.16 g/ml from samples A and B (13). The HCV-like particles of 55-65 nm in diameter showing specific gold labeling when treated with the rabbit polyclonal anti-HCV E2 antibody are shown in Fig. 2A and B. Antibody haloes and their specific binding to goat anti-rabbit IgG colloidal gold particles (10 nm) can be observed in samples A (Fig. 2A) and B (Fig. 2B) but not in sample C or D. Antibody haloes and specific gold labeling were not observed when the normal rabbit serum and the anti-vaccinia virus Lister strain serum was used as the primary antibody in samples A (Fig. 2C) and B. The mixture of five clones of anti-HCV E2 antibodies (159, 260, 305 and 1905) also produced specific gold labeling of an HCV-like particle (Fig. 2D and E). This type of specific reaction was confirmed in samples A (Fig. 2D) and B (Fig. 2E) but not in sample C or D. In Fig. 2D an HCV particle with a visible inner core structure of 35 nm in diameter was also labeled with staphylococcal Protein A conjugated gold
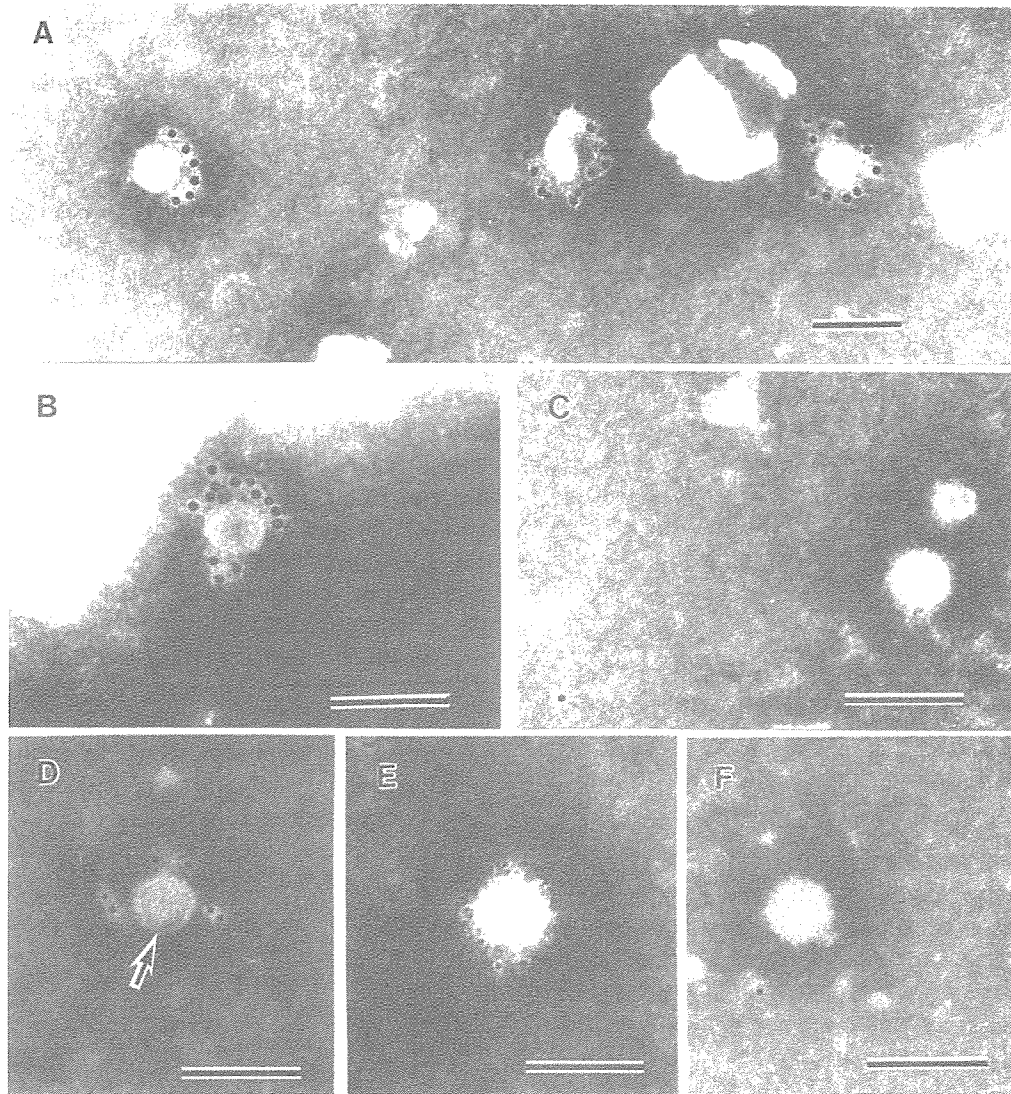
Figure 2. Immunogold electron micrographs of 55-65 nm HCV particles using rabbit polyclonal anti-HCV E2 antibody (RR6) and monoclonal anti-HCV E2 antibodies. HCV-like particles from sample A in (A), (C) and (E), and sample B in (B), (D) and (F) are shown. In (A) and (B), HCV-like particles were reacted with RR6 at a dilution of 1:100, and their antibody haloes were identified by binding to goat anti-rabbit IgG-conjugated colloidal gold particles (10 nm) at a dilution of 1:20. (C) Controls were prepared using rabbit polyclonal antibody to vaccinia virus Lister strain at a dilution of 1:100, following reaction with goat anti-rabbit IgG colloidal gold particles (10 nm) at a dilution of 1:20. In (D) and (E), HCV-like particles were reacted with a mixture of five monoclonal anti-HCV E2 antibodies, at a dilution of 1:10 and staphylococcal Protein A-conjugated colloidal gold particles (5 nm) at a dilution of 1:20. Specific labeling of gold particles on the surface of HCV-like particles can be noted. (D) An HCV-like particle with a visible inner core (indicated by an arrow) can be detected. (F) Controls were prepared using mouse monoclonal antibody to human blood type A antigen. The bars, 100 nm.

particles (5 nm). No specific gold labeling occurred in the presence of mouse monoclonal antibody to human blood type A antigen (Fig. 2F). The HCV-like particles specifically reacted with polyclonal and monoclonal antibodies to the HCV E2 glycoprotein.

Colocalization of the HCV E1 and E2 glycoproteins on the virion surface. When double labeling with different size colloidal gold was performed using monoclonal HCV E1 antibodies and the rabbit anti-HCV E2 polyclonal antibody (RR6), both staphylococcal Protein A-conjugated colloidal gold particles (5 nm) and goat anti-rabbit IgG colloidal gold particles (10 nm) were observed on the surface of the 55 nm HCV particle (Fig. 3A). Moreover, double labeling using the monoclonal HCV E2 antibodies and the rabbit anti-HCV E1 polyclonal antibody (RR2) also produced specific 5 nm and

10 nm gold labeling (Fig. 3B). Specificity of the immunogold labeling was confirmed using the mouse monoclonal antibody to the human blood type A antigen and protein A-conjugated colloidal gold particles (5 nm), and then using rabbit polyclonal antibody to vaccinia virus Lister strain and goat anti-rabbit IgG colloidal gold particles (10 nm) as negative controls, or by omitting the primary antibody. These negative control tests showed no specific gold labeling in 55-65 nm HCV-like particles with delicate surface spike-like projections (Fig. 3C). Both the HCV E1 and E2 glycoproteins colocalized on the surface of HCV virion.

Discussion

Recently, two *in vitro* HCV replication systems have been developed using an infectious HCV genotype 1b cDNA (23)
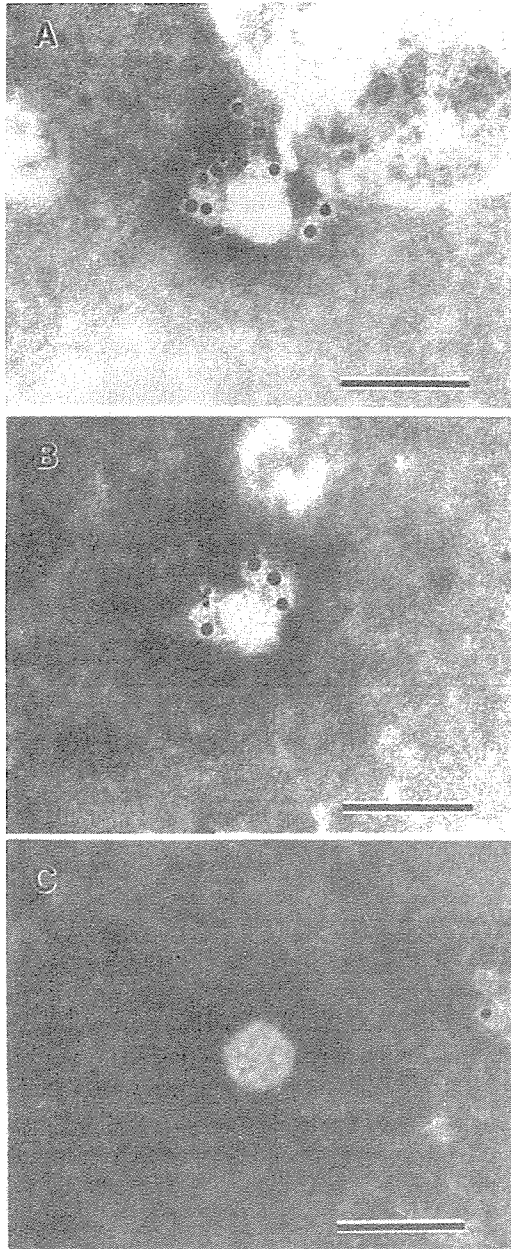
Figure 3. Immunogold electron micrographs of 55-65 nm HCV particles by double labeling with anti-HCV E1 and anti-HCV E2 antibodies. HCV-like particles from sample A are shown. (A) HCV-like particles were treated with a mixture of four monoclonal anti-HCV E1 antibodies at a dilution of 1:10 and staphylococcal Protein A-conjugated colloidal gold particles (5 nm) at a dilution of 1:20, and then with rabbit polyclonal anti-HCV E2 antibody (RR6); antibody haloes were identified by treating with goat anti-rabbit IgG-conjugated colloidal gold particles (10 nm) at a dilution of 1:20. (B) An HCV particle was detected using a mixture of five monoclonal anti-HCV E2 antibodies at a dilution of 1:10 and protein A-conjugated colloidal gold particles (5 nm) at a dilution of 1:20, and rabbit polyclonal anti-HCV E1 antibody (RR2) at a dilution of 1:100 and goat anti-rabbit IgG-conjugated colloidal gold particles (10 nm) at a dilution of 1:20. (C) Controls were prepared using mouse monoclonal antibody to human blood type A antigen at a dilution of 1:10, followed by treatment with Protein A-conjugated colloidal gold particles (5 nm) at a dilution of 1:20, treatment with rabbit polyclonal antibody to vaccinia virus Lister strain at a dilution of 1:100, and with goat anti-rabbit IgG colloidal gold particles (10 nm) at a dilution of 1:20. The bars, 100 nm.

and subgenomic replicons of the JFH1 genotype 2a strain (24). Heller et al (23) described an in vitro HCV replication system that is capable of producing viral particles in culture medium. A full-length HCV construct, CG1b of genotype 1b, known to be infectious (25), was placed between two ribozymes designed to generate the exact 5' and 3' ends of HCV after cleavage. After transfection into a human hepatoma cell line (Huh7), HCV-like particles, approximately 50 nm in diameter, increased in number and secreted into the culture medium. Sucrose density gradient centrifugation of the culture medium revealed colocalization of HCV RNA and structural proteins in a fraction at a density of 1.16 g/ml. HCV-like particles were observed in a fraction at a density of 1.16 g/ml. Wakita et al (24) developed subgenomic replicons of the HCV genotype 2a JFH1 strain cloned from an individual with fulminant hepatitis (26). After transfection into Huh7 cells, HCV particles, of approximately 55 nm in diameter, increased in number and secreted into the culture medium. These particles had a density of 1.15-1.17 g/ml in a 10-60% sucrose density gradient. HCV particles with an electron-dense inner core of 30-35 nm in diameter were identified by immunogold EM using monoclonal anti-HCV E2 antibody. Both studies showed that free HCV particles were about 55 nm spherical particles, had a density of about 1.16 g/ml and a 30-35 nm inner core. The morphology and the density of free HCV particles were quite consistent with our previous study (13). In Fig. 2, we demonstrate that the HCV E2 glycoprotein localized on the surface of 55-65 nm HCV particles containing a 30-35 nm inner core. The indirect immunogold electron microscopy detected immuno-gold-labeling in anti-HCV E2 antibody haloes surrounding the virions; haloes were produced by antigen-antibody reactions on the surface of virus-like particles, and they are good markers to discriminate HCV particles from other particles. In this way, the morphology of HCV virion can also be elucidated. Furthermore, our structural analysis of the HCV E1 and E2 envelope glycoproteins on HCV virions revealed that both HCV E1 and E2 envelope glycoproteins colocalize on the surface of virions in human plasma samples (Fig. 3).

The envelope glycoproteins have been shown to assemble into a noncovalent E1E2 heterodimer that is retained in the endoplasmic reticulum (27). This heterodimer is believed to be the prebudding form of an HCV glycoprotein complex (28). The E1E2 complex has been proposed as a functional subunit of HCV virions (11,12), and the E1E2 heterodimer is thought to be the functional unit of the HCV spike; low pH may induce dissociation leading to homooligomerization of the active form of the fusion protein (29,30). To date, it is known that both HCV E1 and E2 envelope glycoproteins are essential for receptor binding, host-cell entry, and membrane fusion (31,32). The HCV E2 glycoprotein also contains the binding site for CD81, a tetraspanin expressed on hepatocytes and B lymphocytes; CD81 is thought to function as a cellular receptor or coreceptor for the virus (33). Among the cellular factors mediating HCV entry into hepatocytes are tetraspanin CD81 (34-38), the human scavenger receptor SR-B1 (38,39), and probably the receptor for low density lipoproteins (40,41). However, the precise role of each receptor in HCV entry is still unclear and no vaccine is presently available. Further morphological studies on the binding site for CD81, the receptor SR-B1, and the receptor for low density lipoproteins of HCV virions from human plasma samples should be carried out.

In conclusion, both the HCV E1 and E2 glycoproteins are simultaneously present on the surface of the virion, providing definitive evidence that both the E1 and E2 envelope glycoproteins constitute the outer coat of fine spike-like projections of the HCV particle.

Acknowledgement

References

1. Lauer GM and Walker BD: Hepatitis C virus infection. N Engl J Med 345: 41-52, 2001.
2. Lindenbach BD and Rice CM: *Flaviviridae*: the viruses and their replication. In: Fields Virology. Knipe DM and Howley PM (eds). Lippincott Williams & Wilkins, Philadelphia, pp991-1042, 2001.
3. Alter MJ: Epidemiology of hepatitis C. Hepatology 26 (Suppl 1): 62-65, 1997.
4. Montella M, Crispo A, Izzo F, *et al*: HCV and hepatocellular carcinoma: A case-control study in an area of hyperendemicity. Int J Mol Med 6: 571-574, 2000.
5. Fanning LJ: The Irish paradigm on the natural progression of hepatitis C virus infection: an investigation in a homogeneous patient population infected with HCV 1b. Int J Mol Med 9: 179-184, 2002.
6. Nagao Y, Tanaka K, Kobayashi K, Kumashiro R, Sata M: A cohort study of chronic liver disease in an HCV hyperendemic area of Japan: a prospective analysis for 12 years. Int J Mol Med 13: 257-265, 2002.
7. Kato N, Hijikata M, Ootsuyama Y, *et al*: Molecular cloning of the human hepatitis C virus genome from Japanese patients with non-A non-B hepatitis. Proc Natl Acad Sci USA 87: 9524-9528, 1990.
8. Takamizawa A, Mori C, Fuke I, *et al*: Structure and organization of the hepatitis C virus genome isolated from human carriers. J Virol 65: 1105-1113, 1991.
9. Reed KE and Rice CM: Overview of hepatitis C virus genome structure, polyprotein processing, and protein processing, and protein properties. Curr Top Microbiol Immunol 244: 55-84, 2000.
10. Kohara M, Tsukiyama-Kohara K, Maki N, *et al*: Expression and characterization of glycoprotein gp35 of hepatitis C virus using recombinant vaccinia virus. J Gen Virol 73: 2313-2318, 1992.
11. Dubuisson J, Hsu HH, Cheung RC, Greenberg HB, Russell DG and Rice CM: Formation and intracellular localization of hepatitis C virus envelope glycoprotein complexes express by recombinant vaccinia and Sindbis viruses. J Virol 68: 6147-6160, 1994.
12. Ralston R, Thudium K, Berger K, *et al*: Characterization of hepatitis C virus envelope glycoprotein complexes expressed by recombinant vaccinia viruses. J Virol 67: 6753-6761, 1993.
13. Kaito M, Watanabe S, Tsukiyama-Kohara K, *et al*: Hepatitis C virus particle detected by immunoelectron microscopic study. J Gen Virol 75: 1755-1760, 1994.
14. Watanabe S, Kaito M and Kohara M: Immunoelectron microscopic characterization of HCV. In: Methods in Molecular Medicine, vol. 19: Hepatitis C protocols. Lau JYN (ed). Humana Press, Totowa, NJ, pp279-285, 1998.
15. Fujita N, Kaito M, Ishida S, *et al*: Paraformaldehyde protects of Hepatitis C Virus particles during ultracentrifugation. J Med Virol 63: 108-116, 2001.
16. Kaito M, Watanabe S, Kohara M, Tsukiyama-Kohara K, Ishida S, Takeo M, Tanaka H, Horiike S, Naoki F, Iwasa M, Gabazza EC, Ikoma J and Adachi Y: Hepatitis C virus particles detected by immunogold electron microscopy. In: Science, Technology and Education of Microscopy: an Overview. Mendez-Vilas A (ed). Vol. 2, Formatex, Badajoz, pp490-498, 2003.
17. Ishida S, Kaito M, Kohara M, *et al*: Hepatitis C virus core particle detected by immunoelectron microscopy and optical rotation technique. Hepatol Res 20: 335-347, 2001.
18. Simmonds P, McOmish F, Yap PL, *et al*: Sequence variability in the 5' non-coding region of hepatitis C virus: identification of a new virus type and restrictions on sequence diversity. J Gen Virol 74: 661-668, 1993.
19. Kaneko S, Murakami S, Unoura M and Kobayashi K: Quantitation of hepatitis C virus RNA by competitive polymerase chain reaction. J Med Virol 37: 278-282, 1992.
20. Yoshioka K, Kakumu S, Wakita T, *et al*: Detection of hepatitis C virus by polymerase chain reaction and response to interferon-α therapy: relationship to genotypes of hepatitis C virus. Hepatology 16: 293-299, 1992.
21. Fubahashi S, Itamura S, Iinuma H, Nerome K, Sugimoto M and Shida H: Increased expression *in vivo* and *in vitro* of foreign genes directed by A-type inclusion body hybrid promoters in recombinant vaccinia viruses. J Virol 65: 5584-5588, 1991.
22. Matsuura Y, Harada S, Suzuki R, *et al*: Expression of processed envelope protein of hepatitis C virus in mammalian and insect cells. J Virol 66: 1425-1431, 1992.
23. Heller T, Saito S, Auerbach J, *et al*: An *in vitro* model of hepatitis C virion production. Proc Natl Acad Sci USA 102: 2579-2583, 2005.
24. Wakita T, Pietschmann, Kato T, *et al*: Production of infectious hepatitis C virus in tissue culture from a cloned viral genome. Nat Med 11: 791-796, 2005.
25. Thomson M, Nascimbeni M, Gozales S, Murthy KK, Rehermann B and Liang TJ: Emergence of a distinct pattern of viral mutations in chimpanzees infected with a homogeneous inoculum of hepatitis C virus. Gastroenterology 121: 1226-1230, 2001.
26. Kato T, Furusaka A, Miyamoto M, *et al*: Sequence analysis of hepatitis C virus isolated from a fulminant hepatitis patient. J Med Virol 64: 334-339, 2001.
27. Deleersnyder V, Pillez A, Wychowski C, *et al*: Formation of native hepatitis C virus glycoprotein complexes. J Virol 71: 697-704, 1997.
28. Dubuisson J: Folding, assembly and subcellular localization of hepatitis C virus glycoproteins. Curr Top Microbiol Immunol 242: 135-148, 2000.
29. Op De Beeck A, Voisset C, Bartosch B, *et al*: Characterization of functional hepatitis C virus envelope glycoproteins. J Virol 78: 2994-3002, 2004.
30. Lavillette D, Bartosch B, Nourrisson D, *et al*: Hepatitis C virus glycoproteins mediated low pH-dependent membrane fusion with liposomes. J Biol Chem 281: 3909-3017, 2006.
31. Bartosch B, Dubuisson J and Cosset FL: Infectious hepatitis C pseudoviruses containing functional E1E2 envelope protein complexes. J Exp Med 197: 633-642, 2003.
32. Drummer HE and Poumbourios P: Hepatitis C virus glycoprotein E2 contains a membrane-proximal heptad repeat sequence that is essential for E1E2 glycoprotein heterodimerization and viral entry. J Biol Chem 279: 30066-30072, 2004.
33. Pileri P, Uematsu Y, Campagnoli S, *et al*: Binding of hepatitis C virus to CD81. Science 282: 938-941, 1998.
34. Yagnik AT, Lahm A, Meola A, *et al*: A model for the hepatitis C virus envelope glycoprotein E2. Proteins 40: 355-366, 2000.
35. Hsu M, Zhang J, Flint M, *et al*: Hepatitis C virus glycoproteins mediate pH-dependent cell entry of pseudotyped retroviral particles. Proc Natl Acad Sci USA 100: 7271-7276, 2003.
36. Cormier EG, Tsamis F, Kajumo F, Durso RJ, Gardner JP and Dragic T: CD81 is an entry coreceptor for hepatitis C virus. Proc Natl Acad Sci USA 101: 7270-7274, 2004.
37. Bartosch B, Vitelli A, Granier C, *et al*: Cell entry of hepatitis C virus requires a set of co-receptors that include the CD81 tetraspanin and the SR-B1 scavenger receptor. J Biol Chem 278: 41624-41630, 2003.
38. Zhang J, Randall G, Higginbottom A, Monk P, Rice CM and McKeaking JA: CD81 is required for hepatitis C virus glycoprotein-mediated viral infection. J Virol 78: 1448-1455, 2004.
39. Scarselli E, Ansuini H, Cerino R, *et al*: The human scavenger receptor class B type I is a novel candidate receptor for the hepatitis C virus. EMBO J 21: 5017-5025, 2002.
40. Agnello V, Abel G, Elfahal M, Knight GB and Zhang QX: Hepatitis C virus and other flaviviridae viruses enter cells via low density lipoprotein receptor. Proc Natl Acad Sci USA 96: 12766-12771, 1999.
41. André P, Komurian-Pradel F, Deforges S, *et al*: Characterization of low- and very-low-density hepatitis C virus RNA-containing particles. J Virol 76: 6919-6928, 2002.

Original Research

Imaging Living Mice Using a 1-T Compact MRI System

Yusuke Inoue, MD,[1]* Yukihiro Nomura, MS,[1] Tomoyuki Haishi, PhD,[2] Kohki Yoshikawa, MD,[3] Takahiro Seki, PhD,[4] Kyoko Tsukiyama-Kohara, PhD,[4] Chieko Kai, PhD,[4] Toshiyuki Okubo, MD,[1] and Kuni Ohtomo, MD[5]

Purpose: To determine the feasibility of imaging living mice with a 1-T compact MRI system and investigate appropriate imaging techniques for use in routine animal experiments.

Materials and Methods: An MRI system consisting of a 1-T permanent magnet and compact console was used. Images of the entire trunks of living mice were obtained on the system using a T1-weighted three-dimensional fast low-angle shot (3D FLASH) sequence, and image quality was evaluated in relation to imaging techniques.

Results: Restraint of respiratory motion improved the image quality. Decreasing the slice thickness reduced artificial inhomogeneity in signal intensity (SI). Substantial effects of TR and FA on image quality were also demonstrated. With the determined techniques, images covering the entire trunk with a voxel size of 0.26 × 0.26 × 0.52 mm were acquired in an acquisition time of five minutes 28 seconds and a total experiment time of <20 minutes, and various organs and subcutaneous tumors were clearly visualized.

Conclusion: The compact MRI system provides images of living mice with acceptable quality in a reasonable time. Considering its convenience, it appears to be suitable for use in routine mouse experiments.

Key Words: magnetic resonance imaging; mouse; 3D FLASH; imaging technique; permanent magnet
J. Magn. Reson. Imaging 2006;24:901–907.
© 2006 Wiley-Liss, Inc.

MEDICAL IMAGING TECHNOLOGIES, including magnetic resonance imaging (MRI), computed tomography (CT), single photon emission computed tomography (SPECT), and positron emission tomography (PET), are increasingly used for small-animal experiments. Conventional methods of studying animal models require that the animals be killed, and do not allow for serial observations in a given animal. Noninvasive imaging permits investigators to perform short- or long-term repetitive assessments of an individual animal to study anatomical and functional changes related to such things as disease progression, therapeutic effect, and pharmacokinetics. Each animal can be used as its own control, leading to greater reliability of the obtained results even when a small number of animals are used.

MRI can provide three-dimensional (3D) information about both anatomy and function with no radiation exposure, and is recognized as a powerful modality for small-animal experiments (1–4). However, high cost and low research accessibility may preclude the use of MRI in routine experiments (4,5). For imaging small objects, such as mice, high spatial resolution is critically important. To obtain sufficient signal from a small voxel, instruments dedicated to small animals or small samples are commonly used. Such MRI units generally have a small bore and a superconducting magnet of high field strength (≥4 T). Although they can provide sufficient signal for high-resolution imaging, these units often require a large space for installation. Cryogen refills, which are needed to maintain the superconducting magnet, are troublesome, especially for a specific pathogen-free (SPF) animal facility that restricts entry to prevent biological contamination. Some authors have reported the use of a 1.5-T clinical scanner and a dedicated small-animal coil (6–8). However, the time available for animal experiments is limited on a clinical scanner, and imaging of disease-model animals on a clinical unit may cause cross-contamination between animals and patients.

Efforts have been made to improve systems using high-field superconducting magnets for convenience. The use of active shielding can depress the fringe magnetic field, and a refrigeration system can be installed to reduce the frequency of cryogen refills. A compact MRI system that uses a 1-T permanent magnet was recently developed, and high-resolution images of fixed mice were obtained (9). Both the magnet and console of the

901